




RESEARCH ARTICLE

Intrinsic connectivity network dynamics in PTSD during amygdala downregulation

Andrew A. Nicholson^{1,2,3,4}  | Daniela Rabellino^{2,3,4}  | Maria Densmore^{2,3} | Paul A. Frewen^{1,5} | Christian Paret⁶  | Rosemarie Klutsch⁶ | Christian Schmahl⁶ | Jean Théberge^{2,3,7,8,9} | Tomas Ros¹⁰ | Richard W. J. Neufeld^{1,2,5} | Margaret C. McKinnon^{4,11,12} | Jeffrey P. Reiss² | Rakesh Jetly¹³ | Ruth A. Lanius^{1,2,3}

¹Department of Neuroscience, Western University, London, Ontario, Canada

²Department of Psychiatry, Western University, London, Ontario, Canada

³Department of Imaging, Lawson Health Research Institute, London, Ontario, Canada

⁴Homewood Research Institute, Guelph, Ontario, Canada

⁵Department of Psychology, Western University, London, Ontario, Canada

⁶Department of Psychosomatic Medicine and Psychotherapy, Central Institute of Mental Health Mannheim, Medical Faculty Mannheim/Heidelberg University, Mannheim, Germany

⁷Department of Medical Imaging, Western University, London, Ontario, Canada

⁸Department of Medial Biophysics, Western University, London, Ontario, Canada

⁹Department of Diagnostic Imaging, St. Joseph's Healthcare, London, Ontario, Canada

¹⁰Laboratory of Neurology and Imaging of Cognition, Department of Neuroscience, University of Geneva, Geneva, Switzerland

¹¹Mood Disorders Program, St. Joseph's Healthcare, Hamilton, Ontario, Canada

¹²Department of Psychiatry and Behavioural Neuroscience, McMaster University, Hamilton, Ontario, Canada

¹³Canadian Forces, Health Services, Ottawa, Ontario, Canada

Correspondence

Ruth A. Lanius, University Hospital, Windermere Road, PO Box 5339, London, ON N6A 5A5, Canada.

Email: ruth.lanius@lhsc.on.ca

Funding information

Canadian Institute for Health Research; Canadian Institute for Veteran Health Research; Health Research; General Dynamics Land Systems; Canadian Institutes of Health Research

Abstract

Posttraumatic stress disorder (PTSD) has been associated with a disturbance in neural intrinsic connectivity networks (ICN), including the central executive network (CEN), default mode network (DMN), and salience network (SN). Here, we conducted a preliminary investigation examining potential changes in ICN recruitment as a function of real-time fMRI neurofeedback (rt-fMRI-NFB) during symptom provocation where we targeted the downregulation of neural response within the amygdala—a key region-of-interest in PTSD neuropathophysiology. Patients with PTSD ($n = 14$) completed three sessions of rt-fMRI-NFB with the following conditions: (a) *regulate*: decrease activation in the amygdala while processing personalized trauma words; (b) *view*: process trauma words while not attempting to regulate the amygdala; and (c) *neutral*: process neutral words. We found that recruitment of the left CEN increased over neurofeedback runs during the *regulate* condition, a finding supported by increased dlPFC activation during the *regulate* as compared to the *view* condition. In contrast, DMN task-negative recruitment was stable during neurofeedback runs, albeit was the highest during *view* conditions and increased (normalized) during *rest* periods. Critically, SN recruitment was high for both the *regulate* and the *view* conditions, a finding potentially indicative of CEN modality switching, adaptive learning, and increasing threat/defense processing in PTSD. In conclusion, this study provides provocative, preliminary evidence that downregulation of the amygdala using rt-fMRI-NFB in PTSD is associated with dynamic changes in ICN, an effect similar to those observed using EEG modalities of neurofeedback.

Andrew A Nicholson and Daniela Rabellino contributed equally to this study.

KEYWORDS

amygdala, brain connectivity, central executive network, default mode network, salience network, emotion, fMRI neurofeedback, independent component analysis, intrinsic connectivity networks, posttraumatic stress disorder

1 | INTRODUCTION

Posttraumatic stress disorder (PTSD) is a psychiatric illness estimated to occur in approximately 25% of individuals exposed to or witnessing a traumatic event (Santiago et al., 2013). PTSD is characterized by a constellation of symptoms including vivid re-experiencing of traumatic events, avoidance, alterations in cognitions and mood, and hyperarousal (APA, 2013) that together have been linked to a number of biological changes, including alterations in large-scale intrinsic neural networks (Akiki, Averill, & Abdallah, 2017; Krause, Ben, Mander, & Greer, 2017; Lanius, Frewen, Tursich, Jetly, & McKinnon, 2015; Menon, 2011; Rabellino et al., 2015; Shalev, Liberzon, & Marmar, 2017; Shang et al., 2014; Yehuda et al., 2015). In the human brain, three intrinsic connectivity networks (ICN) have been identified as central to the understanding of psychiatric illness and higher cognitive function (Menon, 2011): the central executive network (CEN), default mode network (DMN), and salience network (SN).

The CEN is a frontoparietal and cerebellar network (centered around the dorsolateral prefrontal cortex [dlPFC]) that is crucial to the cognitive control of thought, emotion, working memory, and behavior (Akiki et al., 2017; Habas et al., 2009; Koechlin & Summerfield, 2007; Miller & Cohen, 2001; Petrides, 2005; Seeley et al., 2007). The DMN, which consists of the posterior cingulate cortex (PCC), ventromedial prefrontal cortex (vmPFC), hippocampus, and cortical midline/parietal structures, is active predominantly at rest and is critical to autobiographical self-referential processing, emotion regulation, social cognition, and future-oriented thinking (Buckner, Andrews-Hanna, & Schacter, 2008; Greicius, Krasnow, Reiss, & Menon, 2003; Qin & Northoff, 2011; Spreng, Mar, & Kim, 2008). Finally, the SN is anchored by the dorsal anterior cingulate cortex (dACC), insula, and the amygdala and is involved in the detection of personally salient internal and external stimuli to direct behavior/arousal; it also plays a key role in interoceptive processing (Dosenbach et al., 2007; Seeley et al., 2007; Sridharan, Levitin, & Menon, 2008). Critically, not only have the activation and the recruitment of these ICNs been shown to be aberrant in PTSD, but also these changes have been related to the psychopathology and symptom presentation of the disorder, including cognitive dysfunction (CEN) (Block et al., 2017; Cisler, Steele, Smitherman, Lenow, & Kilts, 2013; St. Jacques, Kragel, & Rubin, 2013), altered self-referential processing (DMN) (Bluhm et al., 2009; Daniels et al., 2010), and dysregulated arousal/interoceptive processing (SN) (Akiki et al., 2017; Birn, Patriat, Phillips, Germain, & Herringa, 2014; Cisler et al., 2014; Daniels et al., 2010; Fonzo et al., 2013; Kennis, Rademaker, van Rooij, Kahn, & Geuze, 2015; Lanius et al., 2015; Menon, 2011; Qin et al., 2012; Rabellino et al., 2015; Shang et al., 2014; Tursich et al., 2015; Yehuda et al., 2015).

The anterior insula of the SN is thought to mediate dynamic switching between the CEN and the DMN, reflecting a change between externally oriented attention and higher-order cognitive processing (CEN) and internal self-reflective functioning (DMN) (Menon & Uddin, 2010; Seeley et al., 2007; Sridharan et al., 2008). Importantly, both the dynamic switching function of the anterior insula/SN (Daniels et al., 2010) and the functional connectivity of the anterior insula with the amygdala and other SN regions (Birn et al., 2014; Cisler et al., 2013, 2014; Fonzo et al., 2013; Nicholson et al., 2016; Rabinak et al., 2011; Shang et al., 2014; Simmons, Norman, Spadoni, & Strigo, 2013; Sripada et al., 2012; Tursich et al., 2015) appear to be disrupted in PTSD. These alterations extend to the functioning of the CEN, where previous studies report decreased recruitment and functional connectivity within the CEN among patients with PTSD during autobiographical memory recall (St. Jacques et al., 2013) and facial emotion processing (Cisler et al., 2013), in addition to during working memory tasks where the DMN is recruited inappropriately (Daniels et al., 2010). These alterations within the CEN are thought to underlie some of the cognitive and emotion regulatory dysfunctions observed in PTSD (Akiki et al., 2017; Frewen, Brown, Steuwe, & Lanius, 2015; Lanius et al., 2015; McKinnon et al., 2016; Shalev et al., 2017). Finally, studies examining the intrinsic functional connectivity of the DMN among patients with PTSD at rest reveal broadly decreased coupling between the PCC, vmPFC, and other DMN structures (Bluhm et al., 2009; Chen & Etkin, 2013; Kennis et al., 2015; Miller et al., 2017; Qin et al., 2012; Shang et al., 2014; Sripada et al., 2012), often in significant association with PTSD symptoms (Birn et al., 2014; Jin et al., 2014; Lanius, Bluhm, et al., 2010; Tursich et al., 2015; Zhou et al., 2012; but also see pediatric PTSD, Patriat et al., 2016). In addition, aberrant connectivity within the DMN has been associated with PTSD symptoms during facial emotion processing (Cisler et al., 2013) and autobiographical memory recall (St. Jacques et al., 2013). In conjunction with ICNs, key subcortical nodes, such as the amygdala, are shown repeatedly to be dysregulated in PTSD, where the majority of patients with PTSD exhibit amygdala hyperactivation and altered functional connectivity to key ICN hubs, including the dlPFC, insula, dACC, and PCC (Aghajani et al., 2016; Birn et al., 2014; Brown et al., 2014; Bruce et al., 2013; Etkin & Wager, 2007; Fonzo et al., 2010; Hopper, Frewen, van der Kolk, Lanius, 2007; Nicholson et al., 2015; Nicholson, Sapru, et al., 2016; Patel, Spreng, Shin, & Girard, 2012; Pitman et al., 2012; Rabinak et al., 2011; Shalev et al., 2017; Shin & Liberzon, 2010; Sripada, King, Garfinkel, et al., 2012; Stevens et al., 2013; Yehuda et al., 2015).

Observations of these altered patterns of neural functioning within patients with PTSD have driven efforts to develop novel

treatment interventions that target the functioning of intrinsic networks (Lanius et al., 2015). Notably, EEG-neurofeedback (EEG-NFB) targeting cortical alpha oscillations was shown to plastically alter connectivity within the SN and DMN (Kluetsch et al., 2014; Ros et al., 2013), while also normalizing amygdala functional connectivity (Nicholson et al., 2016), in association with acute symptom decreases among PTSD patients (Kluetsch et al., 2014). Real-time fMRI neurofeedback (rt-fMRI-NFB) is a similar form of neurofeedback that allows the recipient to modulate neural activation, but using BOLD fMRI signal (Brühl et al., 2014; Keynan et al., 2016; Paret et al., 2014; Paret et al., 2016; Paret et al., 2016; Young et al., 2014; Young, Siegle, Zotev, Phillips, & Misaki, 2017; Zotev et al., 2011, 2016, 2018). In our previous rt-fMRI-NFB proof-of-concept study in PTSD, we demonstrated that successful amygdala downregulation during symptom provocation was associated with a normalization of activity within the prefrontal cortex; here, prefrontal, insula, and anterior cingulate cortex activation was correlated negatively to PTSD symptoms and the amygdala displayed bi-directional effective connectivity to the dlPFC during neurofeedback regulation (Nicholson et al., 2016). In healthy individuals, the functional connectivity of ICNs has been shown to be enhanced via dlPFC based rt-fMRI-NFB training, where most of the observed changes implicated the insula/SN, suggesting that the insula plays a critical role in the organization of ICN during neurofeedback regulation (Zhang, Yao, Shen, Yang, & Zhao, 2015). Elsewhere, direct amygdala regulation via rt-fMRI-NFB has been shown to affect activation in CEN prefrontal areas involved in emotion regulation, as well as enhance amygdala-PFC connectivity (Koush et al., 2013; Paret et al., 2014; Paret, Kluetsch, et al., 2016; Zotev et al., 2011) and SN amygdala-rostral ACC coupling (Zotev et al., 2011) as compared to sham. Notably, however, dynamics of the three main ICNs during amygdala downregulation via rt-fMRI-NFB have not yet been examined in PTSD.

Accordingly, we conducted a preliminary investigation to determine if downregulating the amygdala using rt-fMRI-NFB would lead to plastic changes in ICNs in patients with PTSD, an effect observed previously using EEG-NFB. We conducted ICN analyses on an expanded sample from our original proof-of-concept rt-fMRI-NFB study (Nicholson, Rabellino, et al., 2016) investigating task-relatedness (recruitment of each network) during neurofeedback, which is indicative of a temporal correlation to the task. Collectively, the novel contribution of the current study is the examination of intrinsic network dynamics in patients with PTSD during amygdala downregulating neurofeedback. Based on previous work (Bluhm et al., 2009; Daniels et al., 2010; Lanius et al., 2015; Rabellino et al., 2015), we predicted that downregulating the amygdala and PTSD emotional states during symptom provocation would lead to a concomitant decrease in task-negative ICN recruitment (i.e., DMN), as well as an increase in executive functioning, task-positive ICN recruitment (i.e., CEN and dlPFC) among patients with PTSD. We also predicted increased SN recruitment during neurofeedback, indicative of CEN/DMN modality switching and threat/defense processing.

2 | METHODS

2.1 | Participants

The sample consisted of 14 patients with PTSD (see Table 1 for demographic and clinical characteristics of the study sample), where an analysis on a portion of the sample ($n = 10$) had been published previously in our proof-of-concept rt-fMRI-NFB study (Nicholson, Rabellino, et al., 2016). Exclusion criteria for participants with PTSD included: noncompliance with 3 T fMRI safety standards, a history of head injury with loss of consciousness, significant untreated medical illness, neurological disorders, pervasive developmental disorders, and pregnancy. Further clinical exclusion criteria for PTSD patients included a history of bipolar disorder or schizophrenia, and alcohol or substance dependence/abuse not in sustained full remission within 6 months prior to participation in the study. Participants were assessed using the DSM-IV Structured Clinical Interview (SCID) (First et al., 1997), the Clinician Administered PTSD Scale (CAPS-5) (Weathers et al., 2013), Beck's Depression Inventory (BDI) (Beck et al., 1997), the Childhood Trauma Questionnaire (CTQ) (Bernstein et al., 2003), and the Multiscale Dissociation Inventory (MDI) (Briere et al., 2005). In addition, to assess state changes in PTSD symptoms, participants completed the Response to Script Driven Imagery (RSDI) Scale (Hopper et al., 2007) after each of the four fMRI runs (Table 1), which consisted of the following subscales: dissociation, hyperarousal, avoidance, and reliving. All scanning took place at the Lawson Health Research Institute in London, Ontario, Canada. The research ethics board at the University of Western Ontario approved the current study, and all participants provided written informed consent.

TABLE 1 Demographic and clinical information

Measure	PTSD ($n = 14$)
Age	$M = 48.1 \pm 9.8$
Sex	Females = 9
CAPS-5 Total	31.4 ± 9.7
CTQ	56.7 ± 23.6
BDI	26.6 ± 13.2
MDI-DENG	14.2 ± 4.9
MDI-DEPR	10.5 ± 6.4
MDI-DERL	10.7 ± 6.2
MDI-ECON	12.9 ± 5.4
MDI-MEMD	11.6 ± 5.4
MDI-IDDIS	8.3 ± 5.3
Current medication	$n = 11$
RSDI total run 1	13.4 ± 6.29
RSDI total run 2	13.2 ± 9.8
RSDI total run 3	12.1 ± 8.6
RSDI total transfer run	11.3 ± 8.9

CAPS = clinician administered PTSD scale; CTQ = childhood trauma questionnaire; BDI = Beck's depression inventory; MDI = multiscale dissociation inventory; DENG = disengagement; DEPR = depersonalization; DERL = derealization; ECON = emotional constriction; MEMD = memory disturbance; IDDIS = identity dissociation; RSDI = response to script driven imagery scale.

2.2 | Experimental conditions, visual feedback, and instructions

The same experimental protocol that was implemented in our previous study was used here (Nicholson, Rabellino, et al., 2016). Specifically, patients were instructed to *downregulate the feeling center of their brain*, that is, to decrease bars on the thermometer denoting activation within the bilateral amygdala. To elicit unbiased regulatory strategies, specific instruction on how to regulate the brain region-of-interest (ROI) was not provided (Nicholson, Rabellino, et al., 2016; Paret et al., 2014; Paret, Kluetsch, et al., 2016). During neurofeedback training trials, average bilateral amygdala activation was displayed in the form of two identical thermometers on the left and right side of the screen inside the scanner. Here, the bars on the thermometer increased/decreased as BOLD signal increased/decreased in the amygdala, respectively. Patients were informed that baseline amygdala activation was denoted by the orange line on the thermometer (Figure 1). Patients were first provided with written instructions, followed by a single trial example within the scanner.

Our neurofeedback protocol consisted of three conditions: (a) *regulate*, (b) *view*, and (c) *neutral* (Figure 1). During the *regulate* condition, patients were asked to decrease bars on the thermometer (activity within the amygdala) while viewing a personalized trauma word (Nicholson, Rabellino, et al., 2016). During the *view* condition, patients were asked to respond naturally to their personalized trauma word while not attempting to regulate amygdala activation. Similar to the *view* condition, *neutral* trials consisted of asking patients to respond naturally to personalized neutral words. Our experimental design consisted of three consecutive neurofeedback training runs and one transfer run in which patients received the same three conditions without neurofeedback from the thermometer (to assess learning effects immediately after training). Instructions were presented for 2 s before each condition; each condition lasted for 24 s and conditions were separated by an inter-trial fixation

cross interval (10 s). Before each run, we first collected an initial rest scan for 18 s, where the first initial rest corresponded to the baseline rest (henceforth called the *initial baseline rest* condition), and the subsequent rest periods denote resting activation before runs 2, 3, and 4 (henceforth called *initial rest* conditions). An experimental run lasted about 9 min and consisted of 15 trials (five of each condition, counterbalanced). Critically, personalized trauma and neutral words were selected by patients and matched on subjective units of distress to control for between-subject variability. These stimuli were presented with Presentation software (Neurobehavioral Systems, Berkeley, CA).

One bar on the thermometer display corresponded to 0.2% signal change in the amygdala, consisting of an upper activation range with a maximum of 2.8% signal change and a lower activation range with a maximum of 1.2% signal change (Nicholson, Rabellino, et al., 2016; Paret et al., 2014; Paret, Kluetsch, et al., 2016). Patients were instructed to focus visually on the word during its entire presentation and to view the two thermometers in their peripheral vision. Participants were also informed of the temporal delay that would occur during neurofeedback, corresponding to both the BOLD signal delay and real-time processing of this neural activation. Latency of neurofeedback processing was equal to the TR (2 s) plus the time needed for real-time calculation/visual display by the presentation software (about half a second). Finally, when a neurofeedback run was completed, patients were asked to rate their perceived ability to regulate their emotion center.

2.3 | Delineation and BOLD processing of the amygdala for real-time neurofeedback

In order to present real-time neurofeedback of the amygdala through the thermometer display, anatomical scans were first imported into BrainVoyager (version QX2.4, Brain Innovations, Maastricht, Netherlands), skull-stripped and then transformed into Talairach space. Subsequently, normalization parameters were loaded into

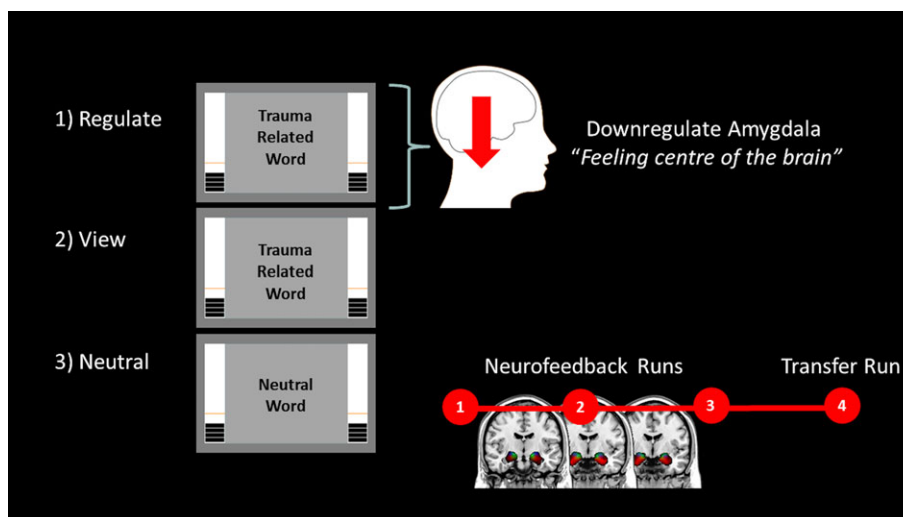


FIGURE 1 Real-time fMRI amygdala neurofeedback experimental design. Patients with PTSD were instructed to downregulate neurofeedback thermometer bars, denoting amygdala activation, on *regulate* trials only. Personalized trauma words were presented in the scanner for *regulate* and *view* conditions, while neutral words were presented for the *neutral* conditions. During *view* and *neutral* conditions, patients with PTSD were instructed to respond naturally to words, while not attempting to regulate their amygdala activation. Our experiment consisted of three consecutive sessions of neurofeedback training, followed by one transfer run without neurofeedback immediately after. Before each condition, there was an initial rest period [Color figure can be viewed at wileyonlinelibrary.com]

TurboBrainVoyager (TBV) (version 3.0, Brain Innovations, Maastricht, Netherlands). Motion correction features and spatial smoothing using a 4-mm full-width-half-maximum (FWHM) Gaussian kernel were implemented in TBV, and the initial two volumes of the functional scans were discarded before real-time processing. An anatomical mask of the bilateral amygdala was implemented with the “best voxel selection” tool in TBV to calculate the BOLD signal amplitude of the ROI. This method identified the 33% of voxels with the highest beta-values for the *view* > *neutral* contrast. As previously outlined by Paret et al. (2014, 2016), the voxels were dynamically determined based on: (a) the voxel with the largest beta value; and (b) on the magnitude of deviation from the mean of all condition betas (Goebel, 2014; Nicholson, Rabellino, et al., 2016). This method ensured that there were no differences in the number of voxels used for signal extraction between subjects and was used to account for moderate shifts in the anatomical delineation due to alignment discrepancies across runs/movement-related slice shifts. The first two trials of each neurofeedback run consisted of *view* and *neutral* conditions thereby allowing for initial selection of amygdala voxels based on the *view* > *neutral* contrast, which was updated dynamically throughout training as voxel selection was refined. For each trial, the mean of the last four data points before stimuli onset were taken as a baseline. The signal was smoothed by calculating the mean of the current and the preceding three data points (Nicholson, Rabellino, et al., 2016; Paret et al., 2014, 2016).

2.4 | fMRI image acquisition and preprocessing

We utilized a 3 Tesla MRI Scanner (Trio, Siemens Medical Solutions, Erlangen, Germany) with a 32 channel head coil for brain imaging. Functional whole brain images of the BOLD contrast were acquired with a gradient echo T2* weighted echo-planar-imaging sequence (TE = 30 ms, TR = 2 s, FOV = 192 × 192 mm, flip angle = 80°, in-plane resolution = 3 × 3 mm). One volume of comprised 36 ascending interleaved slices tilted -20° from AC-PC orientation with a thickness of 3 mm and slice gap of 1 mm. Participants' heads were stabilized. The experimental runs comprised 284 volumes each, where T1-weighted anatomical images were acquired with a Magnetization Prepared Rapid Acquisition Gradient Echo sequence (TE = 3.03 ms, TR = 2.3 s, 192 slices and FOV = 256 × 256 mm).

Preprocessing of the functional images was conducted with SPM12 (Wellcome Department of Cognitive Neurology, London, UK). The first four volumes were discarded, and the following standard preprocessing routine was implemented: slice time correction to the middle slice, followed by spatial alignment to the mean image using a rigid body transformation, reslicing, and coregistration of the functional mean image to the anatomical. We then performed segmentation of all tissue types and normalization to the Montreal Neurological Institute (MNI) standard template. Following this step, images were smoothed using a 6 mm kernel FWHM. Finally, to ensure motion correction, we used the Artifact Detection Tool (ART) software package (www.nitrc.org/projects/artifact_detect) to compute regressors accounting for outlier volumes that were in addition to the six movement regressors computed during standard realignment.

2.5 | Statistical analyses

2.5.1 | First-level analysis

Separate sessions were defined for each neurofeedback training run and the transfer run, where all events (initial rest, instructions, fixation, and conditions) were modeled as blocks of brain activation and convolved with the hemodynamic response function. At this stage, functional data was high-pass filtered and serial correlations were accounted for using an autoregressive AR(1) model; moreover, ART software regressors were included as nuisance variables to account for any additional movement artifacts. The three experimental conditions (*regulate*, *view*, and *neutral*) were modeled separately where we also generated the t-contrast *regulate* > *view* on the first level to examine a priori hypotheses.

2.5.2 | Amygdala downregulation analysis

To examine successful downregulation of the amygdala among patients with PTSD, we extracted parameter estimates of the left and right amygdala during the *regulate* and the *view* conditions using rfx-plot software (Glaser, 2009) via anatomical definition from the PickAtlas toolbox (Maldjian et al., 2003). Extracted values were examined in SPSS (version 24, IBM SPSS Statistics Inc., Armonk, NY), where we computed both a 3 (NFB run) × 2 (condition) × 12 (2-s time bins across the 24-s condition) randomized block analysis of variance (ANOVA), separately for both the left and right amygdala.

As we a priori predicted amygdala activation to be lower specifically during the *regulate* as compared to *view* condition for transfer run and all neurofeedback runs, we also computed paired-sample *t* tests on amygdala parameter estimates for the *regulate* as compared with the *view* conditions during the transfer run and each NFB training run. All paired-sample *t*-tests were Bonferroni corrected for multiple comparisons. We also computed a repeated measures ANOVA to investigate how RSDI state scores fluctuate across training and transfer runs.

2.5.3 | Independent component analysis

We performed an independent component analysis (ICA) on the rt-fMRI data with all neurofeedback runs and all subjects, to identify spatially independent networks. ICA was performed using Group ICA Toolbox (GIFT v4.0b). Taking a data-driven approach, the Infomax algorithm was used to identify 31 independent components (ICs) within the data set (St. Jacques et al., 2013), following minimum description length (MDL) criteria. The ICA estimation was repeated 20 times through ICASSO to ensure the reliability of the components (Himberg, Hyva, & Esposito, 2004). The reduced data were decomposed into a series of spatially independent maps and their corresponding time courses, which were then back reconstructed via principal component analysis (PCA) for each subject to produce individual spatial maps (SMs) and the power spectra of the network time courses (TCs). TCs and SMs were converted into z-scores, where the TCs represent the level of coherent activity within a network, and the intensities of the SMs are related to the connectivity and degree of coactivation within a network. This data-driven approach was used instead of using raw canonical templates, as PTSD networks, especially those used during cognitive self-regulation tasks, are likely

different from those in healthy individuals (Rabellino et al., 2015; Shang et al., 2014; Tursich et al., 2015).

Spatial sorting analysis: component identification

After visually inspecting the obtained components for the presence of artifacts, the spatial sorting function in GIFT was used to correlate the SMs of the components to standard network templates. Here, we correlated components to the CEN (left and right masks separately) and SN templates from https://findlab.stanford.edu/functional_ROIs.html (Rabellino et al., 2015; Shirer, Ryali, Rykhlevskaia, Menon, & Greicius, 2012). The DMN mask was derived from the GIFT toolbox (GIFT v4.0b). The rationale for including bilateral hemispheric masks of the CEN was provided by the Stanford University standard template masks of the left and right CEN (https://findlab.stanford.edu/functional_ROIs.html) (Rabellino et al., 2015; Shirer et al., 2012), as well as recent findings that suggest the left CEN is more involved in explicit cognitive emotion regulation and language paradigms, while the right CEN is associated with implicit perceptual, somesthetic, and nociception processing (Heine et al., 2012; Laird et al., 2011; Smith et al., 2009).

Temporal sorting analysis

We utilized a temporal sorting analysis to identify how neurofeedback task-relatedness of the intrinsic network components changed as a function of time. For the temporal sorting analysis, we used each subject's individual design matrix from the first-level analysis in SPM12, which modeled each condition in the experiment. Utilizing the multiple regression temporal sorting function in GIFT, the resultant beta weights denoting component task-relatedness to an experimental condition were then imported into SPSS for statistical analysis. Taking the four components that were found to be moderately correlated to template masks (left and right CEN, DMN, and SN), we first conducted a three-way 4 (network) \times 4 (NFB condition: rest, regulate, view, and neutral) \times 4 (NFB run: 3 training runs and 1 transfer run) repeated measures ANOVA, to evaluate an effect of network and to justify subsequent follow-up comparisons. After observing significant main effects and interactions, we then conducted separate two-way 4 (NFB condition: rest, regulate, view, and neutral) \times 4 (NFB run: three training runs and one transfer run) repeated measures ANOVAs for each network, in addition to follow-up simple main effect tests and pairwise comparisons among means. If the assumption of sphericity was violated, we applied a Huynh-Feldt correction to degrees of freedom. Follow-up comparisons were justified after observing significant main effects and interactions, where all sets of pairwise contrasts were orthogonal.

Analysis of activation within the dlPFC

Finally, we a priori hypothesized that regulating the amygdala via neurofeedback would lead to increased activation and recruitment of the CEN and dlPFC over training runs. Hence, we evaluated a dlPFC region-of-interest analysis within SPM12 to observe changes in activation during neurofeedback within a central hub of the CEN (Zhang, Zhang, Yao, & Zhao, 2015). We defined 10 mm radius spheres around the bilateral dlPFC (MNI coordinates: x, y, z: right = 45, 23, 38; left = -42, 26, 38) (Zhang, Zhang, et al., 2015). Notably, these bilateral coordinates were within the standard network masks used for the spatial

sorting analysis, and were also within our PTSD data-driven components. We analyzed two different one-way ANOVAs for the contrast *regulate* > *view*: (a) an ANOVA including only the neurofeedback training runs; and (b) an ANOVA including the neurofeedback training runs and transfer run. Here, ROI activation was observed under p -FWE < .05, $k = 10$ error protection rate at the voxelwise level (Eklund, Nichols, & Knutsson, 2016). We also conducted follow-up t -tests under the same error protection rate to observe activation during *regulate* trials for neurofeedback training run 3 and the transfer run as compared to neurofeedback training run 1, thus assessing effects of learning across the training trials and transfer run.

3 | RESULTS

3.1 | Amygdala downregulation with neurofeedback

We found that patients with PTSD were able to significantly downregulate bilateral amygdala activation during *regulate* as compared to *view* conditions. Broadly, amygdala parameter estimates were significantly lower for the *regulate* condition during all neurofeedback training runs and the transfer run as compared to the *view* condition and decreased as a function of time within each run.

Specifically, regarding the right amygdala, the 3 (NFB run) \times 2 (NFB condition) \times 12 (2-s time bins across the 24-s condition) randomized ANOVA yielded a significant main effect of condition ($F[1, 13] = 72.88, p < .001$) and time ($F[12, 156] = 2.28, p < .05$) and also a significant condition \times time interaction ($F[12, 156] = 5.25, p < .001$). For the left amygdala, the 3 (NFB run) \times 2 (NFB condition) \times 12 (time bin) randomized ANOVA yielded a significant main effect of condition ($F[1, 13] = 34.46, p < .001$) and time ($F[12, 156] = 4.11, p < .001$) and also a significant condition \times time interaction ($F[12, 156] = 3.28, p < .001$). Then, we tested our *a-priori* directional hypotheses, where we expected amygdala activation to be lower across the transfer run and each NFB training run during the *regulate* as compared to *view* condition. For the right amygdala, we observed significantly lower activation during the *regulate* as compared to the *view* condition for the first NFB training run ($t[13] = -4.65, p < .001$), second NFB training run ($t[13] = -6.05, p < .001$), and third NFB training run ($t[13] = -3.62, p = .003$), as well as the transfer run ($t[13] = -3.43, p = .004$) (Figure 2a,c). Similarly, for the left amygdala, we observed significantly lower activation during the *regulate* as compared to *view* condition for the first NFB training run ($t[13] = -4.54, p = .001$), second NFB training run ($t[13] = -5.36, p < .001$), and third NFB training run ($t[13] = -4.10, p = .001$), as well as the transfer run ($t[13] = -2.94, p = .011$) (Figure 2b,c). RSDI total scores did not differ significantly across training runs and the transfer run when computing a repeated measures ANOVA for the main effect of run.

3.2 | Spatial sorting analysis: component identification

Four artifact-free components showed moderate-to-high correlations with the predefined template networks masks: the left CEN ($r = .35$), right CEN ($r = .50$), DMN ($r = .40$), and the SN ($r = .35$) (Figures 3–6).

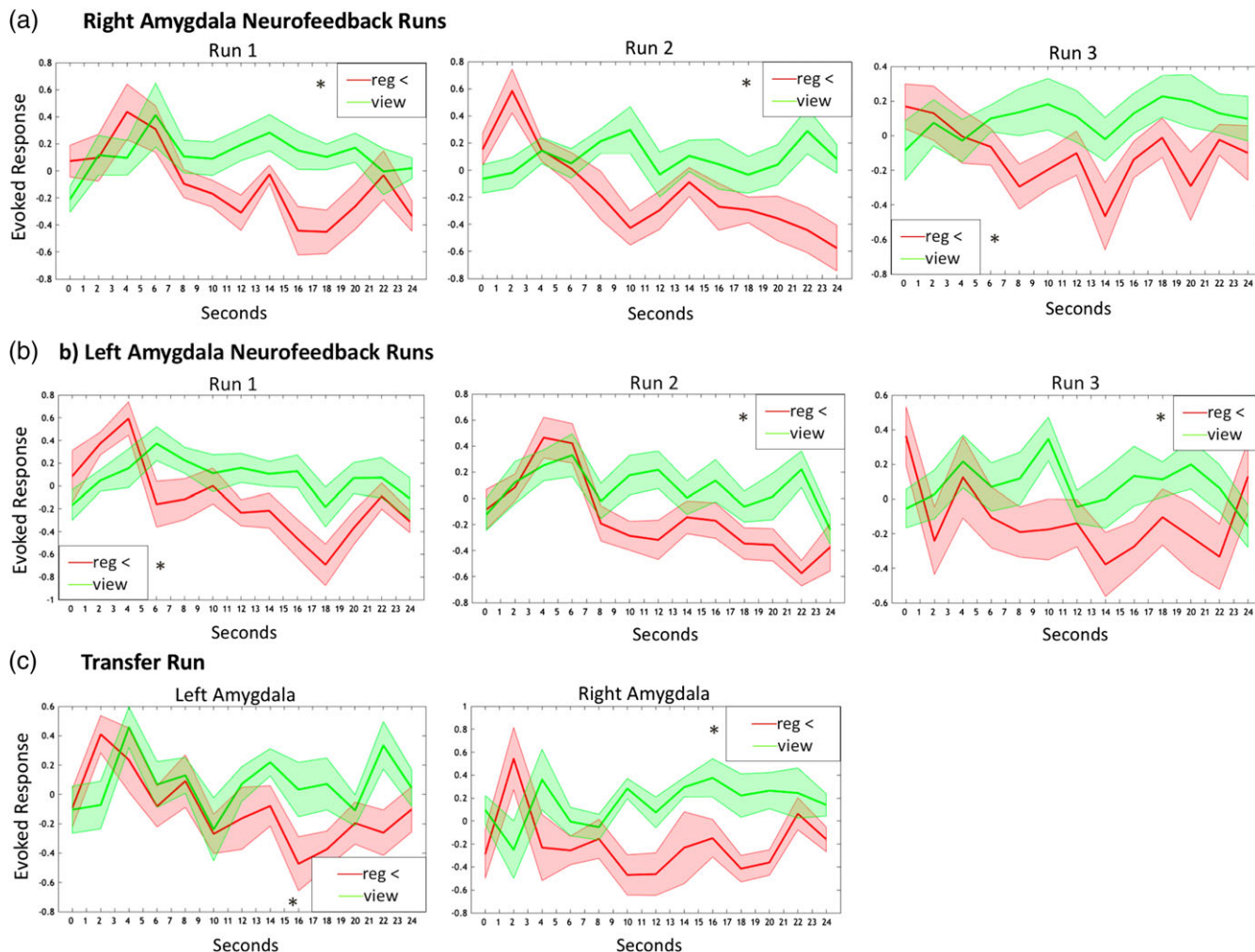


FIGURE 2 (a) Right amygdala parameter estimates corresponding to amygdala activation during neurofeedback training runs for the *view* (solid green line) and *regulate* (solid red line) conditions. (b) Left amygdala parameter estimates corresponding to amygdala activation during neurofeedback training runs for the *view* (solid green line) and *regulate* (solid red line) conditions. (c) Bilateral amygdala parameter estimates corresponding to activation during the transfer run without neurofeedback for the *view* (solid green line) and *regulate* (solid red line) conditions. Shaded red and green regions adjacent to the solid lines indicate standard error of the mean. Statistical thresholds corresponds to *a-priori* paired-sample *t*-tests, comparing amygdala activation during *view* versus *regulate* across the whole condition. Reg = regulate [Color figure can be viewed at wileyonlinelibrary.com]

The left CEN component primarily covered a large prefrontal area in the left hemisphere, including the bilateral dlPFC (superior and middle PFC; Brodmann area [BA] 8, 9). The left CEN component also broadly contained a right cerebellar region (crus I and VIIIb) and the left dorsomedial PFC (BA 8, 9), in addition to the bilateral amygdala, hippocampus, insula, angular gyrus, superior, and inferior parietal lobes (BA 39, 40), superior and middle temporal gyri (BA 39), cuneus (BA 17, 18), precuneus (BA 7), supramarginal gyrus (BA 40), PCC (BA 31), thalamus, and caudate. The right CEN component primarily covered a large prefrontal area in the right hemisphere, including bilateral dlPFC (superior, middle, and inferior PFC; BA 6, 8, 9, 10, 47). The right CEN component also contained a left cerebellar region (crus I and VIIIb), as well as clusters in the right dmPFC (BA 8, 9), bilateral inferior and superior parietal lobes (BA 7, 40), superior and middle temporal gyri (BA 21, 38), cuneus (BA 18), precuneus (BA 7, 19), PCC (BA 23, 24, 31) thalamus, caudate, and the right insula. The DMN component

consisted mainly of anterior regions in the bilateral vmPFC, lateral orbitalfrontal cortex, dmPFC, and inferior frontal gyrus (BA 9, 10, 32, 46, 47), as well as the right hippocampus (BA 19) and bilateral caudate and ACC (BA 24). The SN component comprised mainly a large bilateral region in the dACC, as well as the bilateral insula, periaqueductal gray (PAG), cerebellum (lobule V, VI), superior and middle temporal gyri (BA 22, 38), and the middle frontal gyrus (BA 6, 10). As expected, the amygdala, which is classically not considered part of the CEN, was identified as involved in the CEN as a function of downregulating the amygdala. In addition, among PTSD patients, the CEN was correlated with regions outside the normal canonical network, including the PCC (DMN) and the insula (SN). Taken together with the moderate correlation values observed with template masks, it is probable these results reflect abnormal network functioning and psychopathology in PTSD, where previous studies examining ICNs in PTSD report similar correlation values (Rabellino et al., 2015; Shang et al., 2014; Tursich et al.,

2015). Alternatively, during longer resting-state scans, identified network components may not present as atypical, and instead may simply be linked to the particular experimental conditions in question.

3.3 | Temporal sorting analysis

The three-way 4 (network) \times 4 (NFB condition) \times 4 (NFB run) repeated measures ANOVA, revealed a main effect of network [$F(3, 39) = 22.00, p < .001$], main effect of run [$F(3, 39) = 6.72, p < .001$], a network \times run interaction [$F(9, 117) = 3.63, p < .001$], and a network \times condition interaction [$F(9, 117) = 4.76, p < .001$], justifying the separate examination of each network.

3.3.1 | Left CEN

For the left CEN network, the 4 (NFB condition) \times 4 (NFB run) repeated measures ANOVA revealed a significant main effect of NFB run, and a condition \times run interaction (Tables 2 and 3, Figure 3a,b). Here,

follow-up comparisons demonstrated that left CEN network beta estimates from runs 3 and 4 were significantly higher than run 1 (Figure 3a). With regard to the condition \times run interaction (Table 3, Figure 3b), simple main effects within each condition revealed that for the *rest* condition, the *initial rest* period before runs 3 and 4 were significantly higher than the *initial baseline rest* before run 1; critically, this pattern was held for the *regulate* condition, in which run 4 was significantly higher than run 1. No significant increase was found for the *view* and *neutral* conditions. For the simple main effects within runs, we found that both the *view* and *neutral* conditions beta weights were higher than the *initial baseline rest* and that *view* was also higher than the *regulate* condition; these findings were only significant for NFB run 1.

3.3.2 | Right CEN

For the right CEN network, the 4 (NFB condition) \times 4 (NFB run) repeated measures ANOVA revealed a significant main effect of

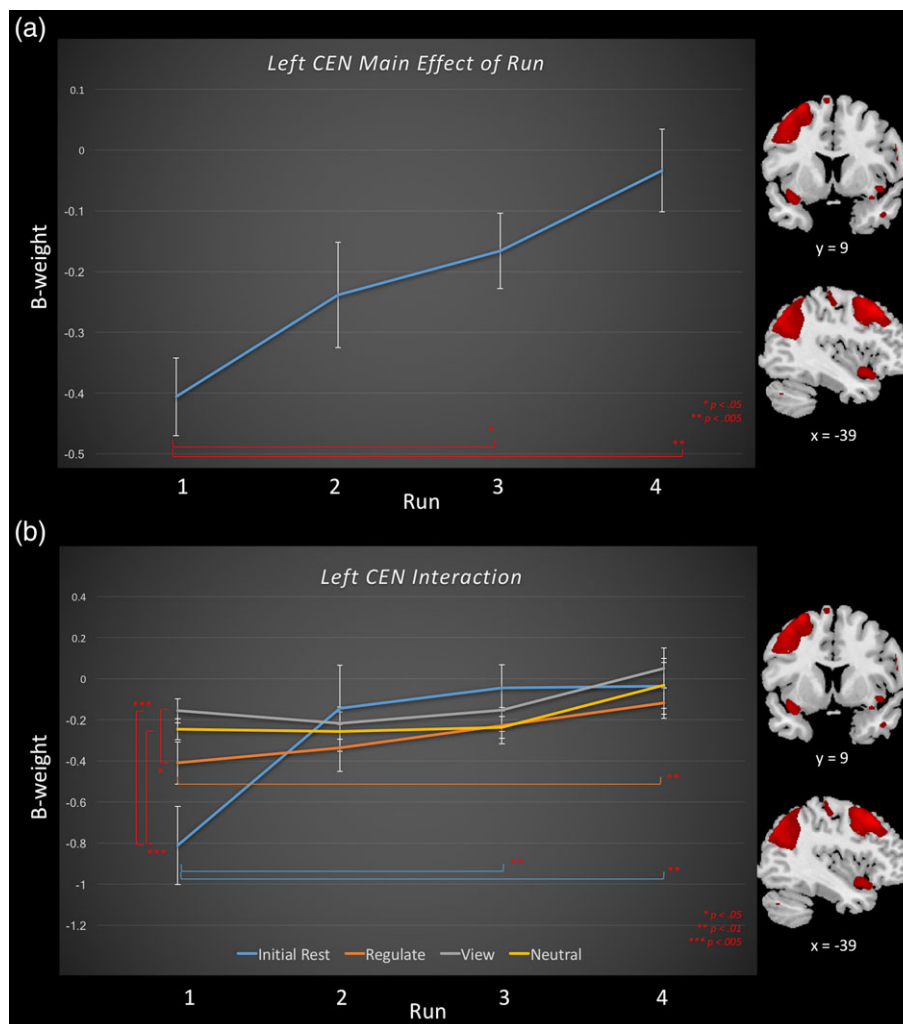


FIGURE 3 Task relatedness of the left central executive network during amygdala downregulating neurofeedback training runs and the transfer run, for the *regulate*, *view*, and *neutral* conditions, as well as the *initial rest*. Runs 1–3 consist of neurofeedback training runs, and run 4 is the transfer run without neurofeedback. Brain images to the right of the graph indicate areas included within the central executive network component. Slice references are in MNI space. Beta weights denote network task-relatedness to an experimental condition. (a) The main effect of run across neurofeedback conditions for the left central executive network. Significant differences between runs are denoted by a red significance bar. (b) The interaction between condition and run for the left central executive network. Simple main effects: significant differences between runs within a condition are denoted by the significance bar that is in the same color as the condition in legend. Significant differences between conditions within a specific run are denoted by a red significance bar [Color figure can be viewed at wileyonlinelibrary.com]

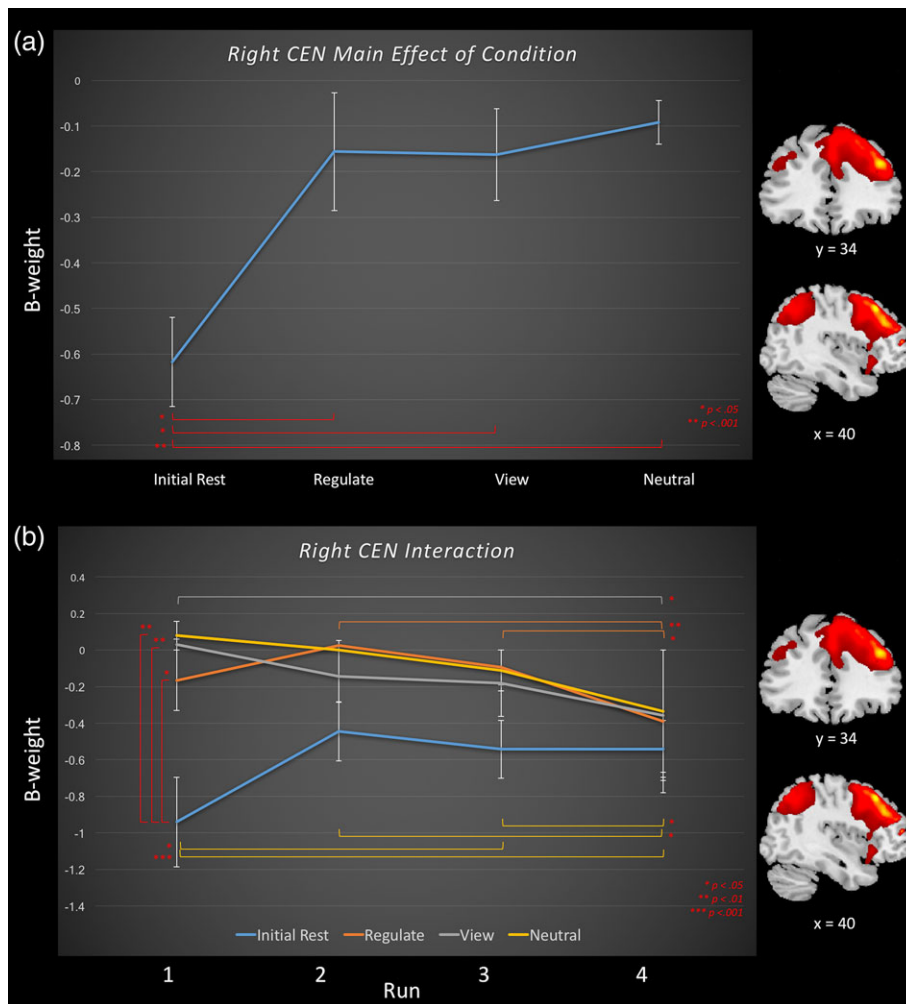


FIGURE 4 Task relatedness of the right central executive network during amygdala downregulating neurofeedback training runs and the transfer run, for the *regulate*, *view*, and *neutral* conditions, as well as for the *initial rest*. Runs 1–3 consist of neurofeedback training runs, and run 4 is the transfer run without neurofeedback. Brain images to the right of the graph indicate areas included within the right central executive network component. Slice references are in MNI space. Beta weights denote network task-relatedness to an experimental condition. (a) The main effect of condition across neurofeedback runs for the right central executive network. Significant differences between conditions are denoted by a red significance bar Bottom. (b) The interaction between condition and run for the right central executive network. Simple main effects: significant differences between runs within a condition are denoted by the significance bar that is in the same color as the condition in legend. Significant differences between conditions within a specific run are denoted by a red significance bar [Color figure can be viewed at wileyonlinelibrary.com]

condition, and a condition \times run interaction (Tables 2 and 3, Figure 4a, b). Follow-up comparisons for the main effect of condition revealed that beta estimates during the *initial rest* condition were significantly lower than for the *regulate*, *view*, and *neutral* conditions. Simple main effects within runs revealed that during run 1, right CEN recruitment was higher for the *regulate*, *view*, and *neutral* conditions as compared to the *initial baseline rest*. Additionally, simple main effects within conditions revealed that recruitment of the right CEN generally decreased for all conditions (*regulate*, *view*, and *neutral*) over runs, except for the *initial rest*, which remained low (Table 3, Figure 4b).

3.3.3 | DMN

With regard to the task-relatedness of the mainly anterior DMN network, the 4 (NFB condition) \times 4 (NFB run) repeated measures ANOVA revealed a significant main effect of condition and run as well as a condition \times run interaction (Tables 2 and 3, Figure 5a,b). The beta estimates for the DMN generally increased over training

across conditions; however, simple main effect analyses revealed that this was only the case for the *initial rest* condition. Follow-up comparisons for the main effect of condition revealed that the DMN network beta estimates were significantly higher for the *view* condition as compared to the *initial rest* and *neutral* conditions. Here, simple main effects within runs showed that during run 1, the *initial baseline rest* was significantly lower than the *regulate*, *view*, and *neutral* conditions, where the *view* condition was also higher than the *neutral* condition.

3.3.4 | SN

For the dACC SN network, the 4 (NFB condition) \times 4 (NFB run) repeated measures ANOVA revealed a significant main effect of condition (Table 2, Figure 6). Follow-up comparisons for the main effect of condition revealed that SN beta estimates were significantly higher for the *regulate* and the *view* conditions as compared to the *initial rest* conditions.

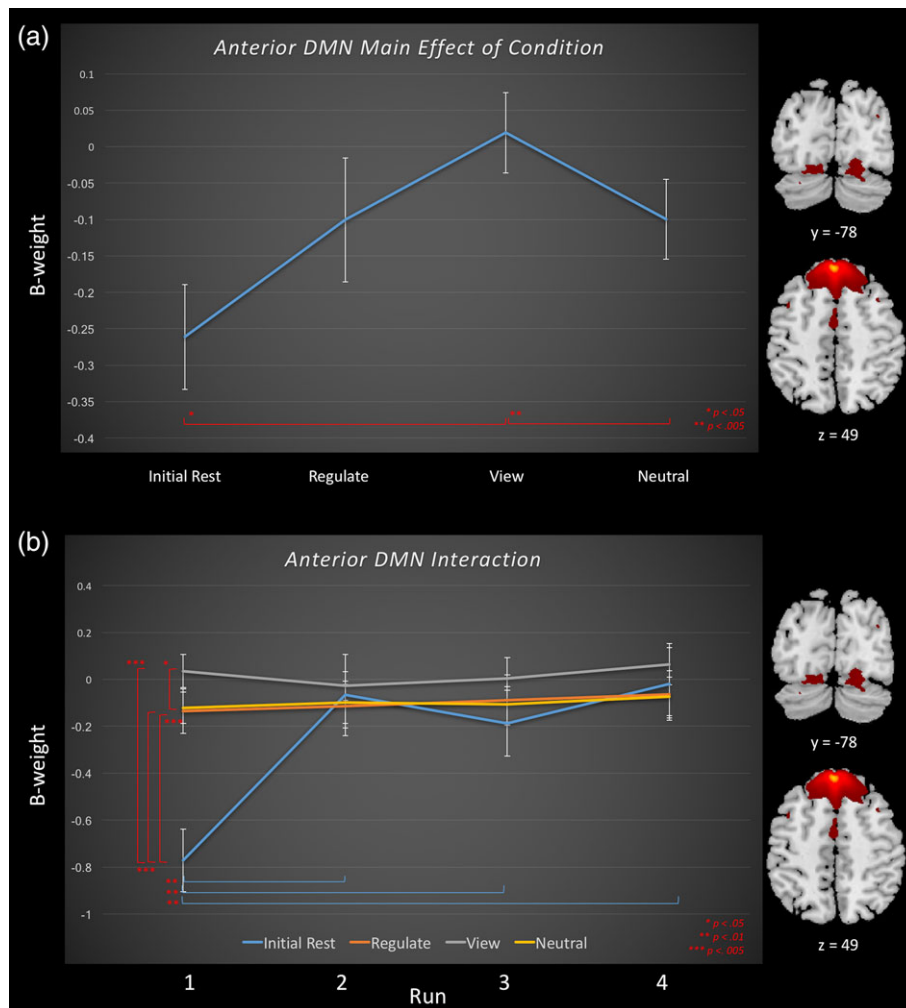


FIGURE 5 Task relatedness of the anterior default mode network across runs during amygdala downregulating neurofeedback for the *regulate*, *view*, and *neutral* conditions, as well as the *initial rest*. Brain images to the right of the graph indicate areas included within the default mode network component. Slice references are in MNI space. Beta weights denote network task relatedness to an experimental condition Top. (a) The main effect of condition across neurofeedback runs for the default mode network. Significant differences between conditions are denoted by a red significance bar Bottom. (b) The interaction between condition and run for default mode network. Simple main effects: significant differences between runs within a condition are denoted by the significance bar that is in the same color as the condition in legend. Significant differences between conditions within a run are denoted by a red significance bar [Color figure can be viewed at wileyonlinelibrary.com]

Analysis of activation within the dlPFC

When investigating the one-way ANOVAs for the *regulate* > *view* contrasts, we found significant activation within the right dlPFC (BA 9) for the main effect of run across the neurofeedback training runs (Table 4). We then conducted follow-up *t* tests under the same error protection rate to observe effects of learning across the training trials and transfer run. Here, we found significantly higher activation within the right dlPFC (BA 9) for training run 3 as compared to training run 1 for the contrast *regulate* > *view* (Table 5). We did not find significantly increased activation in the transfer run as compared to run 1 for the contrast *regulate* > *view*.

4 | DISCUSSION

Our preliminary analysis found that amygdala downregulation via rt-fMRI-NFB was associated with plastic modulation of ICNs implicated previously in PTSD. In our earlier proof-of-concept study, we found

that successful downregulation of the amygdala led to increased activation in prefrontal emotional regulation regions and to increased bi-directional amygdala-PFC connectivity as a function of neurofeedback training, which was negatively correlated to PTSD symptoms in the transfer run (Nicholson, Rabellino, et al., 2016). Interestingly, we have also demonstrated that EEG-NFB targeting DMN-associated (alpha) brain wave oscillations lead to plastic changes within ICNs (Kluetsch et al., 2014), a finding that was further associated with a reorganization of amygdala functional connectivity away from fear processing and defense regions toward prefrontal executive functioning regions (Nicholson, Ros, et al., 2016). In line with these findings, in the present study, we provide a novel demonstration that amygdala downregulation with rt-fMRI-NFB also leads to a plastic modulation of ICNs related to PTSD. Taken together, the current findings are largely consistent with effects observed using EEG-based neurofeedback methods, thus supporting efforts aimed at establishing both treatment and construct validity for this type of intervention.



FIGURE 6 Task relatedness of the salience network during amygdala downregulating neurofeedback training runs and the transfer run, for the *regulate*, *view*, and *neutral* conditions, as well as the *initial rest*. Runs 1–3 consist of neurofeedback training runs, and run 4 is the transfer run without neurofeedback. Displayed is the main effect of condition, and red significance bars indicate differences between conditions averaged across runs. Brain images to the right of the graph indicate areas included within the salience network component. Slice references are in MNI space. Beta weights denote network task relatedness to an experimental condition [Color figure can be viewed at wileyonlinelibrary.com]

4.1 | Amygdala downregulation with neurofeedback

In keeping with results from our previous work (Nicholson, Rabellino, et al., 2016), we observed significantly decreased amygdala activation as a function of time during the *regulate* as compared to *view* condition for all neurofeedback training runs and the transfer run. Here, we did not observe significant changes in state PTSD symptoms across NFB training runs. Therefore, additional studies will be required to assess the effects of repeated sessions of rt-fMRI-NFB on PTSD symptomatology. Critically, future comparisons to secondary/control neurofeedback regions are also urgently needed to establish site specific effects of neurofeedback.

4.2 | Central executive network

We found that learning to downregulate the amygdala during PTSD symptom provocation was associated with unique dynamics within the left and right CEN. Here, we observed increased recruitment of the left CEN as a function of neurofeedback runs. Interestingly, this increase was only apparent for the *regulate* condition, and when comparing the *initial baseline rest* to the *initial rest* period at runs 3 and 4. In addition, we observed decreased recruitment of the right CEN across runs for all conditions (*regulate*, *view*, and *neutral*) except for the *initial rest* condition, which remained low. This suggests that neurofeedback during PTSD symptom provocation is associated with

TABLE 2 Temporal sorting analysis—main effects for the 4 (condition) × 4 (run) repeated measures ANOVAs

Component	4 (condition) × 4 (run) ANOVA	ANOVA main effect statistic	Pairwise comparisons/simple main effects	p value
Left CEN	Main effect of run	$F(3, 39) = 4.90, p = .006$	Run 4 > run 1	<.005
			Run 3 > run 1	<.05
Right CEN	Main effect of condition	<i>ns</i>		
	Main effect of run	$*F(1.36, 17.68) = 6.36, p < .01$	Regulate > rest	<.05
			View > rest	<.05
Neutral > rest	<.001			
DMN	Main effect of run	$F(3, 39) = 3.10, p = .039$	Run 1 < run 2	<.05
			Run 1 < run 3	<.05
			Run 1 < run 4	<.05
			Main effect of condition	$*F(1.74, 22.54) = 3.69, p < .05$
	View > neutral	<.005		
SN	Main effect of run	<i>ns</i>		
	Main effect of condition	$F(3, 39) = 6.91, p = .001$	Regulate > rest	<.005
			View > rest	<.05

Main effect and follow-up comparison results for the 4 Condition × 4 Run repeated measures ANOVA. Runs 1–3 consist of amygdala downregulation neurofeedback training runs, and run 4 is the transfer run without neurofeedback. Asterisks indicate ANOVAs where assumptions of sphericity were violated and a Huynh–Feldt correction was applied. CEN = central executive network; DMN = default mode network; SN = salience network.

TABLE 3 Temporal sorting analysis—interactions and simple main effects for the 4 (condition) × 4 (run) repeated measures ANOVAs

Component analysis	4 (condition) × 4 (run) ANOVA interaction statistic	Simple main effect		Pairwise comparison	p value		
Left CEN	$F(5.11, 66.64) = 2.81, p < .05^*$	Conditions	Rest	Run 1 < run 4	<.01		
					Run 1 < run 3	<.01	
				Regulate	Run 1 < run 4	<.01	
				View	ns		
				Neutral	ns		
			Runs	Run 1	Regulate < view	<.05	
					View > rest	<.005	
					Neutral > rest	<.005	
					Run2	ns	
					Run 3	ns	
					Run 4	ns	
Right CEN	$F(4.20, 54.63) = 2.84, p < .05^*$	Condition	Rest	ns			
			Regulate	Run 2 > run 4	<.01		
				Run 3 > run 4	<.05		
			View	Run 1 > run 4	<.05		
			Neutral	Run 1 > run 3	<.05		
				Run 1 > run 4	<.001		
				Run 2 > run 4	<.05		
				Run 3 > run 4	<.05		
				Runs	Run 1	Regulate > rest	<.05
						View > rest	<.005
						Neutral > rest	<.005
						Run 2	ns
		Run 3	ns				
		Run 4	ns				
DMN	$F(5.43, 70.60) = 3.97, p = .002$	Conditions	Rest	Run 1 < run 2	<.01		
					Run 1 < run 3	<.01	
					Run 1 < run 4	<.01	
				Regulate	ns		
				View	ns		
				Neutral	ns		
			Runs	Run 1	Rest < regulate	<.005	
					Rest < view	<.005	
					Rest < neutral	<.005	
					View > neutral	<.05	
					Run 2	ns	
					Run 3	ns	
		Run 4	ns				
SN	ns						

Interaction and follow-up comparison results for the 4 Condition × 4 Run repeated measures ANOVA. Runs 1–3 consist of amygdala downregulation neurofeedback training runs, and run 4 is the transfer run without neurofeedback. Asterisks indicate ANOVAs where assumptions of sphericity were violated and a Huynh–Feldt correction was applied. CEN = central executive network; DMN = default mode network; SN = salience network.

recruitment of the left versus right CEN, where the CEN is typically deactivated during restful periods (hence the observation of increased left CEN recruitment over the experiment as compared to the *initial baseline rest* at the beginning of the experiment, and right CEN recruitment remaining low throughout). Interestingly, whereas the left CEN is thought to be more involved in explicit cognitive emotion regulation and language paradigms, the right CEN is associated with implicit perceptual, somesthetic, and nociception processing (Heine et al., 2012; Laird et al., 2011; Smith et al., 2009). Notably, whereas the left CEN network

included regions within the amygdala, the right CEN did not, suggesting that the identified left CEN component may be more involved in learning to specifically down regulate the amygdala during trauma provocation in patients with PTSD. We postulate that the observed recruitment of the amygdala within the left CEN network may reflect the critical involvement of this intrinsic network in neurofeedback tasks targeting executive functioning/regulation of the limbic system.

Here, increased recruitment of the left CEN network may serve as a potential mechanism responsible for the observed

TABLE 4 One-way ANOVA for regulate > view ROI analysis

Analysis	Gyrus/sulcus	H	BA	Cluster size	MNI coordinates			F(2, 39)/F(3, 36)	z score	p FWE
					x	y	z			
Main effect of run, across training runs	dIPFC	R	9	44	40	28	44	11.86	3.73	.020
Main effect of run, across training runs and transfer	ns									

One-way analysis of variance for the dIPFC region-of-interest analysis, corresponding to activation during *regulate* as compared to *view* condition (p -FWE < .05 voxelwise corrected, $k = 10$). BA = Brodmann area; FWE = family-wise error protection rate; H = hemisphere; dIPFC = dorsolateral prefrontal cortex.

downregulation of the amygdala as a function of neurofeedback training, as we found that recruitment of the left CEN increased over neurofeedback runs. As noted, this effect was unique to the *regulate* condition, as well as when comparing the *initial baseline rest* to the rests periods before runs 3 and 4. Critically, increased left CEN task-relatedness was not observed for the *view* and *neutral* conditions, which may suggest a central role of the *regulate* condition for increasing left CEN recruitment. In addition, for the first NFB run only, recruitment of the left CEN was significantly less during the *regulate* condition and *initial baseline rest* as compared to the *view* condition. This result may parallel an inappropriate initial decrease in recruitment of executive functioning during the *regulate* condition, which in turn may represent an important neural signature of PTSD associated with poor performance on cognitive tasks (Cisler et al., 2013; Daniels et al., 2010; St. Jacques et al., 2013). Importantly, this effect was reversed over neurofeedback training runs, where left CEN recruitment increased for the *regulate* condition in addition, since PTSD has been shown to involve inappropriate recruitment of DMN regions during tasks that require executive functioning and increased CEN recruitment (Daniels et al., 2010), inclusion of the PCC within the PTSD left and right CENs may be an indication of suboptimal cognitive functioning in PTSD before neurofeedback (Akiki et al., 2017; Frewen et al., 2015; Lanius et al., 2015; McKinnon et al., 2016; Shalev et al., 2017).

In key support of our ICA findings, activation within the dIPFC was condition specific, displaying increased activation during *regulate* as compared to *view* conditions. Critically, this right dIPFC region was also part of both the left and right CEN data-driven components from our ICA analysis. Notably, the bilateral dIPFC is involved in executive functioning and in emotion regulation (Etkin, Büchel, & Gross, 2015). On balance, this finding points further toward significant recruitment of emotion regulation regions, perhaps as a function of learning to downregulate the amygdala during trauma triggers via neurofeedback and, overall, supports the enhanced left CEN functioning observed in our ICA analysis. Nonetheless, future studies should incorporate comparisons to secondary neurofeedback regions as an internal control necessary to confirm this hypothesis. Moreover, the inclusion of

regions in the opposite hemisphere of the brain when referencing a specific hemisphere network, albeit very small relative to the dominant contralateral clusters, is reflective of the moderate correlations scores that emerged between standard healthy template masks and the networks identified by our ICA analysis (i.e., the left CEN including small clusters in the right hemisphere). Taken together, these findings suggest that there is not a perfect separation of central executive functioning in one hemisphere versus the other during our neurofeedback task in patients with PTSD.

The current results support previous rt-fMRI-NFB studies investigating self-regulation of the amygdala when compared to sham regions, which was shown to similarly activate regions in the PFC associated with executive functioning, as well as to enhance amygdala-PFC connectivity (Koush et al., 2013; Paret et al., 2014; Paret, Kluetsch, et al., 2016; Zotev et al., 2011). In addition, our previous study investigating EEG-NFB in patients with PTSD revealed that neurofeedback was also associated with increased PFC connectivity with the amygdala that was concurrent with symptom alleviation. Our CEN findings are further consistent with emotion modulation models of PTSD that characterize PTSD symptom manifestation as resulting primarily from failed top-down inhibition of the PFC and rostral ACC on the amygdala in the majority of PTSD patients (Aupperle, Melrose, Stein, & Paulus, 2012; Koch et al., 2016; Lanius, Vermetten, et al., 2010; Nicholson et al., 2017; Patel et al., 2012; Pitman et al., 2012). Indeed, PTSD hyperarousal symptoms have been correlated to negative medial PFC-amygdala coupling (Sadeh, Spielberg, Warren, Miller, & Heller, 2014) during PTSD emotional processing (Bruce et al., 2013), and a recent dynamic casual modeling analysis by our group suggests that PTSD patients show bottom-up limbic effective connectivity from amygdala complexes and the PAG, toward to PFC, as compared to healthy controls and the dissociative subtype of PTSD (Nicholson et al., 2017).

4.3 | Anterior default mode network

The rt-fMRI-NFB task was associated with stable recruitment of task-negative DMN across the *regulate*, *view*, and *neutral*

TABLE 5 Follow up t test for regulate > view

Analysis	Gyrus/sulcus	H	BA	Cluster size	MNI coordinates			T(14)	z score	p FWE
					x	y	z			
Run 3 > Run1	dIPFC	R	9	118	38	30	44	4.67	3.51	<.001
Transfer run > run 1	ns									

Follow-up t test comparisons for the both the training and transfer + training one-way ANOVA for the dIPFC region-of-interest (p -FWE < .05 voxelwise corrected, $k = 10$). BA = Brodmann area; FWE = family-wise error protection rate; H = hemisphere; dIPFC = dorsolateral prefrontal cortex.

conditions. Furthermore, we observed increased DMN recruitment during the *initial rest* conditions before NFB runs as compared to the *initial baseline rest*. Studies investigating DMN intrinsic functional connectivity among patients with PTSD at rest generally report decreased coupling between the PCC, vmPFC, and other DMN structures (Bluhm et al., 2009; Chen & Etkin, 2013; Kennis et al., 2015; Miller et al., 2017; Qin et al., 2012; Shang et al., 2014; Sripada, King, Welsh, et al., 2012), where aberrant DMN functioning has been associated with PTSD symptom presentation (Birn et al., 2014; Jin et al., 2014; Lanius, Vermetten, et al., 2010; Tursich et al., 2015; Zhou et al., 2012; but also see pediatric PTSD, Patriat et al., 2016). In addition, altered connectivity within the DMN has also been associated with PTSD symptoms during facial emotion processing (Cisler et al., 2013) and autobiographical memory recall (St. Jacques et al., 2013). The current results suggest a stabilized task-negative DMN in PTSD, as recruitment significantly increased over runs for the *initial rest* conditions. Recruitment during the *view* condition was significantly higher as compared to the *initial baseline rest* and *neutral* conditions, where specifically during run 1 the initial baseline rest condition was significantly lower as compared to all other conditions. This may be indicative of a preliminary suppressed resting DMN during the *initial baseline rest* and *neutral* trials at the beginning of the experiment, characteristic of PTSD patients (Bluhm et al., 2009; Chen & Etkin, 2013; Kennis et al., 2015; Miller et al., 2017; Qin et al., 2012; Shang et al., 2014; Sripada, King, Welsh, et al., 2012). Interestingly, patients with PTSD often inappropriately recruit the DMN instead of the CEN when executive functioning is required, as compared to healthy controls (Daniels et al., 2010). Here, our observation of no significant increases in DMN recruitment during the *regulate* condition may represent a shift away from self-referential/autobiographical memory processing toward more adaptive CEN functioning to regulate the limbic system during symptom provocation, where typically we would expect to see increased DMN recruitment during cognitive tasks in PTSD (i.e., increased recruitment during the *regulate* as compared to *neutral* condition) (Daniels et al., 2010). Provocatively, this characteristic signature of PTSD was not observed during this fMRI neurofeedback task.

Providing additional support for neurofeedback altering amygdala-DMN circuitry, we have shown that decreasing DMN-associated brain waves in PTSD patients using EEG-neurofeedback leads to a normalization of amygdala resting-state functional connectivity away from fear processing and defensive regions toward executive functioning and emotion regulation PFC regions (Nicholson, Ros, et al., 2016). Notably, our DMN network comprised mainly anterior regions, where it is likely that posterior regions such as the PCC that are missing from the DMN component are being incorporated by the malfunctioning CEN in PTSD, as mentioned above. Interestingly, Tursich et al. (2015) found that decreased connectivity within the anterior DMN as well as decreased connectivity between the anterior and posterior DMN was related to depersonalization/derealization symptoms in PTSD. Hence, comparisons to control groups as well as to dissociative subtype PTSD patients, who exhibit additional symptoms of hypoarousal, emotional numbing/detachment, and depersonalization/derealization (APA, 2013), are warranted in future studies.

4.4 | Salience network

Finally, rt-fMRI-NFB was associated with increased SN recruitment during the *regulate* and *view* conditions as compared to the *initial rest* conditions. Indeed, the SN and anterior insula are thought to mediate modality switching between DMN autobiographical self-reflective functioning, and CEN externally oriented attention and higher order cognitive processes (Menon & Uddin, 2010; Seeley et al., 2007; Sridharan et al., 2008). Critically, this anterior insula/SN switching function (Daniels et al., 2010) as well as the functional connectivity of the anterior insula with the amygdala and other SN regions (Birn et al., 2014; Cisler et al., 2013; 2014; Fonzo et al., 2013; Nicholson, Sapru, et al., 2016; Rabinak et al., 2011; Shang et al., 2014; Simmons et al., 2013; Sripada, King, Garfinkel, et al., 2012; Tursich et al., 2015) has been shown to be aberrant in PTSD. Hence, increased SN network recruitment during *regulate* conditions may represent an underlying normalization/switching function associated with the observed increase in left CEN recruitment while patients are self-regulating. Zhang, Yao, et al.'s (2015) finding that the insula plays a critical role in the reorganization of functional connectivity among the three ICNs during dlPFC rt-fMRI-NFB provides additional support for this hypothesis. Furthermore, increased SN activation during the *regulate* and *view* conditions most likely represents increased threat/defense processing during trauma word presentation, as the SN is involved in the detection of personally salient stimuli to direct behavior/arousal and also plays a key role in interoceptive processing (Dosenbach et al., 2007; Seeley et al., 2007; Sridharan et al., 2008), where critically, we do not observe this effect for the *neutral* condition. Hence, increased SN recruitment may also reflect salience processing of the trauma words, where a stronger increase during the *regulate* conditions may also reflect salience of the feedback.

Similarly, we have also shown that normalizing DMN-associated (alpha) brain wave oscillations in PTSD patients via EEG-NFB leads to increased insula/SN connectivity (Kluetsch et al., 2014) and a shift in amygdala connectivity from the PAG and hippocampus toward emotion regulation regions associated with executive functioning (Nicholson, Ros, et al., 2016). Interestingly, the SN network was found to include the PAG, a midbrain region involved in defense (fight-or-flight) and emotional coping responses (Bandler, Keay, Floyd, & Price, 2000; Linnman, Moulton, Barmettler, Becerra, & Borsook, 2012). The PAG displays exacerbated resting-state functional connectivity among PTSD patients, which is thought to be indicative of increased defensive, threat, and fight-or-flight processing (Harricharan et al., 2016; Thome et al., 2016) and may support SN changes in threat-sensitivity circuits contributing to the hypervigilance and hyperarousal symptoms in PTSD (Lanius et al., 2015). Moreover, the dACC has been shown to be hyperactive in PTSD (Akiki et al., 2017; Patel et al., 2012) with increased coupling within the SN during threat processing (Rabellino et al., 2015). Here, designs incorporating repeated session of neurofeedback are needed to investigate if successful amygdala downregulation can also decrease SN activation observed in the *regulate* condition. Taken together, our results indicate increased SN recruitment during the *regulate* and *view* conditions as compared to *initial rest* conditions, which may be indicative of CEN modality switching, adaptive learning, and increasing threat/defense processing in PTSD.

4.5 | Limitations and future directions

Limitations of our preliminary analysis include a small sample size, and lack of control groups that allow us to compare ICN architecture between PTSD patients and healthy individuals. It would be interesting to address regulating ICNs directly as well as target regulation within key ICN hubs (i.e., the PFC, PCC, and insula) in future studies. Additionally, as an internal control, we would like to correlate observed neuronal effects as a result of regulating the amygdala as compared to other regions to draw site specific conclusions (Rance, Ruttorf, Nees, Rudi Schad, & Flor, 2014; Thibault, Lifshitz, & Raz, 2015). Our sample was also not large enough to examine the dissociative subtype of PTSD separately, which is also a future direction of our group. Finally, future studies will need to examine the effects of repeated sessions of rt-fMRI-NFB on state and trait PTSD symptoms.

5 | CONCLUSION

Alterations in the neural circuitry of the amygdala as well as the three main intrinsic connectivity networks, such as CEN, DMN, and SN, have been shown repeatedly to be heavily implicated in the symptom presentation of patients with PTSD. We found that patients with PTSD were successfully able to downregulate amygdala activation during PTSD symptom provocation, which was sustained in a transfer run without neurofeedback. Importantly, we found that recruitment of the left CEN increased over neurofeedback runs, which was corroborated by increased dlPFC activation during the *regulate* as compared to the *view* condition. In addition, SN recruitment was increased during the *regulate* and *view* conditions as compared to *initial rest* conditions, possibly indicative of CEN/DMN modality switching, adaptive learning and increasing threat/defense processing. Critically, DMN task recruitment was found to be stable across the *regulate*, *view*, and *neutral* conditions, and was increased for the *initial rest* conditions, which may be related to stabilized task-negative DMN functioning during cognitive tasks in PTSD and at rest. These results suggest alterations in ICN functioning within PTSD patients during amygdala downregulation via real-time neurofeedback. Importantly, similar modulation of ICNs has been observed with EEG-neurofeedback methods conducted by our group, which speaks to the emerging validity of neurofeedback as an adjunctive treatment. In conclusion, this is the first demonstration that successful downregulation of the amygdala using rt-fMRI-NFB in PTSD is associated with a plastic modulation of ICNs.

ACKNOWLEDGMENTS

This study was funded by Canadian Institutes of Health Research (CIHR), General Dynamics Land Systems, and the Canadian Institute for Veteran Health Research (CIMVHR), and the authors declare no conflicts of interest. Furthermore, this study constitutes original research that has not been previously published or submitted for publication elsewhere.

ORCID

Andrew A. Nicholson  <http://orcid.org/0000-0002-9483-5628>

Daniela Rabellino  <http://orcid.org/0000-0002-3914-7363>

Christian Paret  <http://orcid.org/0000-0002-9225-7182>

REFERENCES

- Aghajani, M., Veer, I. M., van Hoof, M. J., Rombouts, S. A., van der Wee, N. J., & Vermeiren, R. R. (2016). Abnormal functional architecture of amygdala-centered networks in adolescent posttraumatic stress disorder. *Human Brain Mapping, 25*, S637–S638. [https://doi.org/10.1016/S0924-977X\(15\)30904-4](https://doi.org/10.1016/S0924-977X(15)30904-4)
- Akiki, T. J., Averill, C. L., & Abdallah, C. G. (2017). A network-based neurobiological model of PTSD: Evidence from structural and functional neuroimaging studies. *Current Psychiatry Reports, 19*, 81.
- APA. (2013). *Diagnostic and statistical manual of mental disorders* (5th ed.). Arlington, VA: American Psychiatric Publishing.
- Aupperle, R. L., Melrose, A. J., Stein, M. B., & Paulus, M. P. (2012). Executive function and PTSD: Disengaging from trauma. *Neuropharmacology, 62*, 686–694. <https://doi.org/10.1016/j.neuropharm.2011.02.008>
- Bandler, R., Keay, K. A., Floyd, N., & Price, J. (2000). Central circuits mediating patterned autonomic activity during active vs. passive emotional coping. *Brain Research Bulletin, 53*, 95–104.
- Beck, A. T., Guth, D., Steer, R. A., & Ball, R. (1997). Screening for major depression disorders in medical inpatients with the beck depression inventory for primary care. *Behaviour Research and Therapy, 35*, 785–791.
- Bernstein, D. P., Stein, J. A., Newcomb, M. D., Walker, E., Pogge, D., Ahluvalia, T., ... Zule, W. (2003). Development and validation of a brief screening version of the Childhood Trauma Questionnaire. *Child Abuse & Neglect, 27*, 169–190.
- Birn, R. M., Patriat, R., Phillips, M. L., Germain, A., & Herringa, R. J. (2014). Childhood maltreatment and combat posttraumatic stress differentially predict fear-related fronto-subcortical connectivity. *Depression and Anxiety, 31*, 880–892. <https://doi.org/10.1002/da.22291>
- Block, S. R., King, A. P., Sripada, R. K., Weissman, D. H., Welsh, R., & Liberzon, I. (2017). Behavioral and neural correlates of disrupted orienting attention in posttraumatic stress disorder. *Cognitive, Affective, & Behavioral Neuroscience, 17*(2), 422–436.
- Bluhm, R. L., Williamson, P. C., Osuch, E. A., Frewen, P. A., Stevens, T. K., Boksman, K., ... Lanius, R. A. (2009). Alterations in default network connectivity in posttraumatic stress disorder related to early-life trauma. *Journal of Psychiatry & Neuroscience, 34*, 187–194.
- Briere, J., Weathers, F. W., & Runtz, M. (2005). Is dissociation a multidimensional construct? Data from the multiscale dissociation inventory. *Journal of Trauma Stress, 18*, 221–231.
- Brown, V. M., LaBar, K. S., Haswell, C. C., Gold, A. L., Beall, S. K., Van Voorhees, E., ... Morey, R. A. (2014). Altered resting-state functional connectivity of basolateral and centromedial amygdala complexes in posttraumatic stress disorder. *Neuropsychopharmacology, 39*, 361–369. <https://doi.org/10.1038/npp.2013.197>
- Bruce, S. E., Buchholz, K. R., Brown, W. J., Yan, L., Durbin, A., & Sheline, Y. I. (2013). Altered emotional interference processing in the amygdala and insula in women with post-traumatic stress disorder. *NeuroImage Clinical, 2*, 43–49. <https://doi.org/10.1016/j.nicl.2012.11.003>
- Brühl, A. B., Scherpiet, S., Sulzer, J., Stämpfli, P., Seifritz, E., & Herwig, U. (2014). Real-time neurofeedback using functional MRI could improve down-regulation of amygdala activity during emotional stimulation: A proof-of-concept study. *Brain Topography, 27*, 138–148.
- Buckner, R. L., Andrews-Hanna, J. R., & Schacter, D. L. (2008). The brain's default network anatomy, function and relevance to disease. *Annals of the New York Academy of Sciences, 38*, 1–38.
- Chen, A. C., & Etkin, A. (2013). Hippocampal network connectivity and activation differentiates post-traumatic stress disorder from generalized anxiety disorder. *Neuropsychopharmacology, 38*, 1889–1898. <https://doi.org/10.1038/npp.2013.122>
- Cisler, J. M., Steele, J. S., Lenow, J. K., Smitherman, S., Everett, B., Messias, E., & Kilts, C. D. (2014). Functional reorganization of neural

- networks during repeated exposure to the traumatic memory in post-traumatic stress disorder: An exploratory fMRI study. *Journal of Psychiatric Research*, 48, 47–55. <https://doi.org/10.1016/j.jpsychires.2013.09.013>
- Cisler, J. M., Steele, J. S., Smitherman, S., Lenow, J. K., & Kilts, C. D. (2013). Neural processing correlates of assaultive violence exposure and PTSD symptoms during implicit threat processing: A network-level analysis among adolescent girls. *Psychiatry Research: Neuroimaging*, 214, 238–246. <https://doi.org/10.1016/j.pscychresns.2013.06.003>
- Daniels, J. K., McFarlane, A. C., Bluhm, R. L., Moores, K. A., Richard Clark, C., Shaw, M. E., ... Lanius, R. A. (2010). Switching between executive and default mode networks in posttraumatic stress disorder: Alterations in functional connectivity. *Journal of Psychiatry & Neuroscience*, 35, 258–266.
- Dosenbach, N. U. F., Fair, D. A., Miezin, F. M., Cohen, A. L., Wenger, K. K., Dosenbach, R. A., ... Petersen, S. E. (2007). Distinct brain networks for adaptive and stable task control in humans. *Proceedings of the National Academy of Sciences of the United States of America*, 104, 11073–11078.
- Eklund, A., Nichols, T. E., & Knutsson, H. (2016). Cluster failure: Why fMRI inferences for spatial extent have inflated false-positive rates. *Proceedings of the National Academy of Sciences of the United States of America*, 113, 201602413–201607905. <https://doi.org/10.1073/pnas.1602413113>
- Etkin, A., Büchel, C., & Gross, J. J. (2015). The neural bases of emotion regulation. *Nature Reviews. Neuroscience*, 16, 693–700.
- Etkin, A., & Wager, T. D. (2007). Functional neuroimaging of anxiety: A meta-analysis of emotional processing in PTSD, social anxiety disorder and specific phobia. *American Journal of Psychiatry*, 164, 1476–1488.
- First, M. B. (1997). *User's Guide for the Structured Clinical Interview for DSM-IV Axis I Disorders SCID-I: Clinician Version*. Washington, DC: American Psychiatric Press.
- Fonzo, G. A., Flagan, T. M., Sullivan, S., Allard, C. B., Grimes, E. M., Simmons, A. N., ... Stein, M. B. (2013). Neural functional and structural correlates of childhood maltreatment in women with intimate-partner violence-related posttraumatic stress disorder. *Psychiatry Research: Neuroimaging*, 211, 93–103. <https://doi.org/10.1016/j.pscychresns.2012.08.006>
- Fonzo, G. A., Simmons, A. N., Thorp, S. R., Norman, S. B., Paulus, M. P., & Stein, M. B. (2010). Exaggerated and disconnected insular-amygdalar blood oxygenation level-dependent response to threat-related emotional faces in women with intimate-partner violence posttraumatic stress disorder. *Biological Psychiatry*, 68, 433–441. <https://doi.org/10.1016/j.biopsych.2010.04.028>
- Frewen, P. A., Brown, M. F. D., Steuwe, C., & Lanius, R. A. (2015). Latent profile analysis and principal axis factoring of the DSM-5 dissociative subtype. *European Journal of Psychotraumatology*, 1, 1–16.
- Goebel R (2014): Dynamic ROIs. TBV users guide. Retrieved from: <http://download.brainvoyager.com/tbv/TBVUsersGuide/Neurofeedback/-DynamicROIs.html>
- Glascher, J. (2009). Visualization of group inference data in functional neuroimaging. *Neuroinformatics*, (1), 73–82.
- Greicius, M. D., Krasnow, B., Reiss, A. L., & Menon, V. (2003). Functional connectivity in the resting brain: A network analysis of the default mode hypothesis. *Proceedings of the National Academy of Sciences of the United States of America*, 100, 253–258.
- Habas, C., Kamdar, N., Nguyen, D., Prater, K., Beckmann, C. F., Menon, V., & Greicius, M. D. (2009). Distinct cerebellar contributions to intrinsic connectivity networks. *The Journal of Neuroscience*, 29, 8586–8594.
- Harricharan, S., Rabellino, D., Frewen, P., Densmore, M., Théberge, J., McKinnon, M., ... Lanius, R. (2016). fMRI functional connectivity of the periaqueductal gray in PTSD and its dissociative subtype. *Brain and Behavior*, 6, e00579.
- Heine, L., Soddu, A., Gómez, F., Vanhauzenhuysse, A., Tshibanda, L., Thonnard, M., ... Demertzi, A. (2012). Resting state networks and consciousness alterations of multiple resting state network connectivity in physiological, pharmacological and pathological consciousness states. *Frontiers in Psychology*, 3, 295.
- Himberg, J., Hyva, A., & Esposito, F. (2004). Validating the independent components of neuroimaging time series via clustering and visualization. *NeuroImage*, 22, 1214–1222.
- Hopper, J. W., Frewen, P. A., van der Kolk, B. A., Lanius, R. A. (2007). Neural correlates of reexperiencing, avoidance, and dissociation in PTSD: Symptom dimensions and emotion dysregulation in responses to script-driven trauma imagery. *J Traum Stress*, 20, 713–725.
- Jin, C., Qi, R., Yin, Y., Hu, X., Duan, L., Xu, Q., ... Xiang, H. (2014). Abnormalities in whole-brain functional connectivity observed in treatment-naive post-traumatic stress disorder patients following an earthquake. *Psychological Medicine*, 44, 1927–1936.
- Kennis, M., Rademaker, A. R., van Rooij, S. J. H., Kahn, S., & Geuze, E. (2015). Resting state functional connectivity of the anterior cingulate cortex in veterans with and without post-traumatic stress disorder. *Human Brain Mapping*, 36, 99–109.
- Keynan, J. N., Meir-Hasson, Y., Gilam, G., Cohen, A., Jackont, G., Kinreich, S., ... Hendler, T. (2016). Limbic activity modulation guided by fMRI-inspired EEG improves implicit emotion regulation. *Biological Psychiatry*, 80(6), 490–496.
- Kluetsch, R. C., Ros, T., Théberge, J., Frewen, P. A., Calhoun, V. D., Schmah, C., ... Lanius, R. A. (2014). Plastic modulation of PTSD resting-state networks and subjective wellbeing by EEG neurofeedback. *Acta Psychiatrica Scandinavica*, 130, 123–136.
- Koch, S. B. J., van Zuiden, M., Nawijn, L., Frijling, J. L., Veltman, D. J., & Olf, M. (2016). Aberrant resting-state brain activity in posttraumatic stress disorder: A meta-analysis and systematic review. *Depression and Anxiety*, 33(7), 592–605. <https://doi.org/10.1002/da.22478>
- Koechlin, E., & Summerfield, C. (2007). An information theoretical approach to prefrontal executive function. *Trends in Cognitive Sciences*, 11, 229–235.
- Koush, Y., Rosa, M. J., Robineau, F., Heinen, K., Rieger, W. S., Weiskopf, N., ... Scharnowski, F. (2013). Connectivity-based neurofeedback: Dynamic causal modeling for real-time fMRI. *NeuroImage*, 81, 422–430. <https://doi.org/10.1016/j.neuroimage.2013.05.010>
- Krause, A. J., Ben, S. E., Mander, B. A., & Greer, S. M. (2017). The sleep-deprived human brain. *Nature Reviews. Neuroscience*, 18, 404–418. <https://doi.org/10.1038/nrn.2017.55>
- Laird, A. R., Fox, P. M., Eickhoff, S. B., Turner, J. A., Ray, K. L., Mckay, D. R., ... Fox, P. T. (2011). Behavioral interpretations of intrinsic connectivity networks. *Journal of Cognitive Neuroscience*, 23, 4022–4037.
- Lanius, R. A., Bluhm, R. L., Coupland, N. J., Hegadoren, K. M., Rowe, B., Théberge, J., ... Brimson, M. (2010). Default mode network connectivity as a predictor of post-traumatic stress disorder symptom severity in acutely traumatized subjects. *Acta Psychiatrica Scandinavica*, 121, 33–40.
- Lanius, R. A., Frewen, P. A., Tursich, M., Jetly, R., & McKinnon, M. C. (2015). Restoring large-scale brain networks in PTSD and related disorders: A proposal for neuroscientifically-informed treatment interventions. *Acta Psychiatrica Scandinavica*, 1, 1–12.
- Lanius, R. A., Vermetten, E., Loewenstein, R. J., Brand, B., Christian, S., Bremner, J. D., & Spiegel, D. (2010). Emotion modulation in PTSD: Clinical and neurobiological evidence for a dissociative subtype. *The American Journal of Psychiatry*, 167, 640–647.
- Linnman, C., Moulton, E. A., Barmettler, G., Becerra, L., & Borsook, D. (2012). Neuroimaging of the periaqueductal gray: State of the field. *NeuroImage*, 60, 505–522.
- Maldjian, J. A., Laurienti, P. J., Burdette, J. B., & Kraft, R. A. (2003). An automated method for neuroanatomic and cytoarchitectonic atlas-based interrogation of fMRI data sets. *NeuroImage*, 19, 1233–1239.
- McKinnon, M. C., Boyd, J. E., Frewen, P. A., Lanius, U. F., Jetly, R., Richardson, J. D., & Lanius, R. A. (2016). A review of the relation between dissociation, memory, executive functioning and social cognition in military members and civilians with neuropsychiatric conditions. *Neuropsychologia*, 90, 210–234. <https://doi.org/10.1016/j.neuropsychologia.2016.07.017>
- Menon, V. (2011). Large-scale brain networks and psychopathology: A unifying triple network model. *Trends in Cognitive Sciences*, 15, 483–506. <https://doi.org/10.1016/j.tics.2011.08.003>
- Menon, V., & Uddin, L. Q. (2010). Saliency, switching, attention and control: A network model of insula function. *Brain Structure & Function*, 214(5–6), 655–667.

- Miller, D. R., Logue, M. W., Wolf, E. J., Maniates, H., Robinson, M. E., Hayes, J. P., ... Miller, M. W. (2017). Posttraumatic stress disorder symptom severity is associated with reduced default mode network connectivity in individuals with elevated genetic risk for psychopathology. *Depression and Anxiety, 34*(7), 632–640.
- Miller, E. K., & Cohen, J. D. (2001). An integrative theory of prefrontal cortex function. *Annual Review of Neuroscience, 24*, 167–202.
- Nicholson, A., Densmore, M., Frewen, P. A., Théberge, J., Neufeld, R. W. J., McKinnon, M. C., & Lanius, R. A. (2015). The dissociative subtype of posttraumatic stress disorder: Unique resting-state functional connectivity of basolateral and centromedial amygdala complexes. *Neuropsychopharmacology, 40*, 2317–2326.
- Nicholson, A. A., Friston, K. J., Zeidman, P., Harricharan, S., McKinnon, M. C., Densmore, M., ... Lanius, R. A. (2017). Dynamic causal modeling in PTSD and its dissociative subtype: Bottom-up versus top-down processing within fear and emotion regulation circuitry. *Human Brain Mapping, 38*, 5551–5561.
- Nicholson, A. A., Rabellino, D., Densmore, M., Frewen, P. A., Paret, C., Kluetsch, R., ... Lanius, R. A. (2016). The neurobiology of emotion regulation in posttraumatic stress disorder: Amygdala downregulation via real-time fMRI neurofeedback. *Human Brain Mapping, 38*, 541–560. <https://doi.org/10.1002/hbm.23402>
- Nicholson, A. A., Ros, T., Frewen, P. A., Densmore, M., Théberge, J., Kluetsch, R. C., & Lanius, R. A. (2016). Alpha oscillation neurofeedback modulates amygdala complex connectivity and arousal in posttraumatic stress disorder. *NeuroImage Clinical, 12*, 506–516. <https://doi.org/10.1016/j.nicl.2016.07.006>
- Nicholson, A. A., Sapru, I., Densmore, M., Frewen, P. A., Neufeld, R. W. J., Théberge, J., ... Lanius, R. A. (2016). Unique insula subregion resting-state functional connectivity with amygdala complexes in posttraumatic stress disorder and its dissociative subtype. *Psychiatry Research: Neuroimaging, 250*, 61–72. <https://doi.org/10.1016/j.pscychres.2016.02.002>
- Paret, C., Kluetsch, R., Ruf, M., Demirakca, T., Hoesterey, S., Ende, G., & Schmahl, C. (2014). Down-regulation of amygdala activation with real-time fMRI neurofeedback in a healthy female sample. *Frontiers in Behavioral Neuroscience, 8*, 299.
- Paret, C., Kluetsch, R., Zaehring, J., Ruf, M., Demirakca, T., Bohus, M., ... Schmahl, C. (2016). Alterations of amygdala-prefrontal connectivity with real-time fMRI neurofeedback in BPD patients. *Social Cognitive and Affective Neuroscience, 11*(6), 952–960.
- Paret, C., Ruf, M., Fungisai Gerchen, M., Kluetsch, R., Demirakca, T., Jungkunz, M., ... Ende, G. (2016). fMRI neurofeedback of amygdala response to aversive stimuli enhances prefrontal-limbic brain connectivity. *NeuroImage, 125*, 182–188. <https://doi.org/10.1016/j.neuroimage.2015.10.027>
- Patel, R., Spreng, R. N., Shin, L. M., & Girard, T. A. (2012). Neurocircuitry models of posttraumatic stress disorder and beyond: A meta-analysis of functional neuroimaging studies. *Neuroscience and Biobehavioral Reviews, 36*, 2130–2142. <http://linkinghub.elsevier.com/retrieve/pii/S0149763412000930>
- Patriat, R., Birn, R., Keding, T. J., & Heringa, R. J. (2016). NEW RESEARCH Default-Mode Network Abnormalities in Pediatric Posttraumatic Stress Disorder, 55, 319–327.
- Petrides, M. (2005). Lateral prefrontal cortex: Architectonic and functional organization. *Philosophical Transactions of the Royal Society of London, Series B: Biological Sciences, 360*(1456), 781–795.
- Pitman, R. K., Rasmusson, A. M., Koenen, K. C., Shin, L. M., Orr, S. P., Gilbertson, M. W., ... Liberzon, I. (2012). Biological studies of post-traumatic stress disorder. *Nature Reviews. Neuroscience, 13*, 769–787. <https://doi.org/10.1038/nrn3339>
- Qin, L., Wang, Z., Sun, Y., Wan, J., Su, S., Zhou, Y., & Xu, J. (2012). A preliminary study of alterations in default network connectivity in post-traumatic stress disorder patients following recent trauma. *Brain Research, 1484*, 50–56. <https://doi.org/10.1016/j.brainres.2012.09.029>
- Qin, P., & Northoff, G. (2011). NeuroImage how is our self related to midline regions and the default-mode network? *NeuroImage, 57*, 1221–1233. <https://doi.org/10.1016/j.neuroimage.2011.05.028>
- Rabellino, D., Tursich, M., Frewen, P. A., Daniels, J. K., Densmore, M., Théberge, J., & Lanius, R. A. (2015). Intrinsic connectivity networks in post-traumatic stress disorder during sub- and supraliminal processing of threat-related stimuli. *Acta Psychiatrica Scandinavica, 132*, 365–378.
- Rabinak, C. A., Angstadt, M., Welsh, R. C., Kennedy, A. E., Lyubkin, M., Martis, B., & Luan Phan, K. (2011). Altered amygdala resting-state functional connectivity in post-traumatic stress disorder. *Frontiers in Psychiatry, 2*, 62.
- Rance, M., Ruttorf, M., Nees, F., Rudi Schad, L., & Flor, H. (2014). Real time fMRI feedback of the anterior cingulate and posterior insular cortex in the processing of pain. *Human Brain Mapping, 5798*, 5784–5798.
- Ros, T., Théberge, J., Frewen, P. A., Kluetsch, R., Densmore, M., Calhoun, V. D., & Lanius, R. A. (2013). Mind over chatter: Plastic up-regulation of the fMRI salience network directly after EEG neurofeedback. *NeuroImage, 65*, 324–335. <https://doi.org/10.1016/j.neuroimage.2012.09.046>
- Sadeh, N., Spielberg, J. M., Warren, S. L., Miller, G. a., & Heller, W. (2014). Aberrant neural connectivity during emotional processing associated with posttraumatic stress. *Clinical Psychological Science, 2*, 748–755. <https://doi.org/10.1177/2167702614530113>
- Santiago, P. N., Ursano, R. J., Gray, C. L., Pynoos, R. S., Spiegel, D., Lewis-fernandez, R., ... Fullerton, C. S. (2013). A systematic review of PTSD prevalence and trajectories in DSM-5 defined trauma exposed populations: Intentional and non-intentional traumatic events. *PLoS One, 8*, e59236.
- Seeley, W. W., Menon, V., Schatzberg, A. F., Keller, J., Glover, G. H., Kenna, H., ... Greicius, M. D. (2007). Dissociable intrinsic connectivity networks for salience processing and executive control. *The Journal of Neuroscience, 27*, 2349–2356.
- Shalev, A., Liberzon, I., & Marmar, C. (2017). Post-traumatic stress disorder. *The New England Journal of Medicine, 376*, 2459–2469. <https://doi.org/10.1056/NEJMra1612499>
- Shang, J., Lui, S., Meng, Y., Zhu, H., Qiu, C., Gong, Q., ... Zhang, W. (2014). Alterations in low-level perceptual networks related to clinical severity in PTSD after an earthquake: A resting-state fMRI study. *PLoS One, 9*, e96834. <https://doi.org/10.1371/journal.pone.0096834>
- Shin, L. M., & Liberzon, I. (2010). The neurocircuitry of fear, stress, and anxiety disorders. *Neuropsychopharmacology, 35*, 169–191.
- Shirer, W. R., Ryali, S., Rykhlevskaia, E., Menon, V., & Greicius, M. D. (2012). Decoding subject-driven cognitive states with whole-brain connectivity patterns. *Cerebral Cortex, 3*, 158–165.
- Simmons, A. N., Norman, B., Spadoni, D., & Strigo, I. A. (2013). Neurosubstrates of remission following prolonged exposure therapy in veterans with posttraumatic stress disorder. *Psychotherapy and Psychosomatics, 82*, 382–389.
- Smith, S. M., Fox, P. T., Miller, K. L., Glahn, D. C., Fox, P. M., Mackay, C. E., ... Beckmann, C. F. (2009). Correspondence of the brain's functional architecture during activation and rest. *Proceedings of the National Academy of Sciences of the United States of America, 106*(31), 13040–13045.
- Spreng, R. N., Mar, R. A., & Kim, A. S. N. (2008). The common neural basis of autobiographical memory, prospection, navigation, theory of mind, and the default mode: A quantitative meta-analysis. *Journal of Cognitive Neuroscience, 21*(3), 489–510.
- Sridharan, D., Levitin, D. J., & Menon, V. (2008). A critical role for the right fronto-insular cortex in switching between central-executive and default-mode networks. *Proceedings of the National Academy of Sciences of the United States of America, 105*(34), 12569–12574.
- Sripada, R. K., King, A. P., Garfinkel, S. N., Wang, X., Sripada, C. S., Welsh, R. C., & Liberzon, I. (2012). Altered resting-state amygdala functional connectivity in men with posttraumatic stress disorder. *Journal of Psychiatry & Neuroscience, 37*, 241–249.
- Sripada, R. K., King, A. P., Welsh, R. C., Garfinkel, S. N., Wang, X., Sripada, C. S., & Liberzon, I. (2012). Neural dysregulation in posttraumatic stress disorder: Evidence for disrupted equilibrium between salience and default mode brain networks. *Psychosomatic Medicine, 74*(9), 904–911.
- St. Jacques, P. L. S., Kragel, P. A., & Rubin, D. C. (2013). Neural networks supporting autobiographical memory retrieval in posttraumatic stress disorder. *Cognitive, Affective, & Behavioral Neuroscience, 13*(3), 554–566.
- Stevens, J. S., Jovanovic, T., Fani, N., Ely, T. D., Glover, E. M., Bradley, B., & Ressler, K. J. (2013). Disrupted amygdala-prefrontal functional connectivity in civilian women with posttraumatic stress disorder. *Journal of*

- Psychiatric Research*, 47, 1469–1478. <https://doi.org/10.1016/j.jpsychores.2013.05.031>
- Thibault, R. T., Lifshitz, M., & Raz, A. (2015). ScienceDirect the self-regulating brain and neurofeedback: Experimental science and clinical promise. *Cortex*, 74, 247–261. <https://doi.org/10.1016/j.cortex.2015.10.024>
- Thome, J., Densmore, M., Frewen, P. A., Mckinnon, M. C., Th, J., Nicholson, A. A., ... Lanius, R. A. (2016). Desynchronization of autonomic response and central autonomic network connectivity in post-traumatic stress disorder. *Human Brain Mapping*, 38(1), 27–40.
- Tursich, M., Ros, T., Frewen, P. A., Kluetsch, R. C., Calhoun, V. D., & Lanius, R. A. (2015). Distinct intrinsic network connectivity patterns of post-traumatic stress disorder symptom clusters. *Acta Psychiatrica Scandinavica*, 132(1), 29–38.
- Weathers, F. W., Blake, D. D., Schnurr, P. P., Kaloupek, D. G., Marx, B. P., & Keane, T. M. (2013). The clinician-administered PTSD scale for DSM-5 (CAPS-5). The CAPS-5 is available from the National Center for PTSD at www.ptsd.va.gov.
- Yehuda, R., Hoge, C. W., McFarlane, A. C., Vermetten, E., Lanius, R. A., Nievergelt, C. M., ... Hyman, S. E. (2015). Post-traumatic stress disorder. *Nature Reviews Disease Primers*, 1, 15057.
- Young, K. D., Siegle, G. J., Zotev, V., Phillips, R., & Misaki, M. (2017). Randomized clinical trial of real-time fMRI amygdala neurofeedback for major depressive disorder: Effects on symptoms and autobiographical memory recall. *American Journal of Psychiatry*, 174(8), 748–755.
- Young, K. D., Zotev, V., Phillips, R., Misaki, M., Yuan, H., Drevets, W. C., & Bodurka, J. (2014). Real-time fMRI neurofeedback training of amygdala activity in patients with major depressive disorder. *PLoS One*, 9, e88785.
- Zhang, G., Yao, L., Shen, J., Yang, Y., & Zhao, X. (2015). Reorganization of functional brain networks mediates the improvement of cognitive performance following real-time neurofeedback training of working memory. *Human Brain Mapping*, 36, 1705–1715.
- Zhang, Q., Zhang, G., Yao, L., & Zhao, X. (2015). Impact of real-time fMRI working memory feedback training on the interactions between three core brain networks. *Frontiers in Behavioral Neuroscience*, 9, 1–9.
- Zhou, Y., Wang, Z., Qin, L., Wan, J., Sun, Y., Su, S., ... Xu, J. (2012). Early altered resting-state functional connectivity predicts the severity of post-traumatic stress disorder symptoms in acutely traumatized subjects. *PLoS One*, 7, e46833.
- Zotev, V., Krueger, F., Phillips, R., Alvarez, R. P., Simmons, W. K., Bellgowan, P., ... Bodurka, J. (2011). Self-regulation of amygdala activation using real-time fMRI neurofeedback. *PLoS One*, 6, e24522.
- Zotev, V., Phillips, R., Misaki, M., Wong, C. K., Wurfel, B. E., Krueger, F., ... Bodurka, J. (2018). Real-time fMRI neurofeedback training of the amygdala activity with simultaneous EEG in veterans with combat-related PTSD. *NeuroImage: Clinical*, 19, 106–121.
- Zotev, V., Yuan, H., Misaki, M., Phillips, R., Young, K. D., Feldner, M. T., & Bodurka, J. (2016). Correlation between amygdala BOLD activity and frontal EEG asymmetry during real-time fMRI neurofeedback training in patients with depression. *NeuroImage Clinical*, 11, 224–238.

How to cite this article: Nicholson AA, Rabellino D, Densmore M, et al. Intrinsic connectivity network dynamics in PTSD during amygdala downregulation. *Hum Brain Mapp.* 2018;1–18. <https://doi.org/10.1002/hbm.24244>